+

Preamble

Over the years NSSL has been providing technical information to the National Weather Service. This exchange had many forms, from formal reports and algorithms to consultation and supply of radar data in real time to the Weather Services Forecast Office. After the decision to evolve its network of WSR-88Ds to keep pace with emerging knowledge and technology, the NWS provided a spare WSR-88D to NSSL. Hence, NSSL became the principal NOAA Laboratory for evolutionary and revolutionary enhancements of weather radar science and technology. At that time (mid nineties) Doppler Radar and Remote Sensing Research group committed to document in report form all significant innovations, changes, and results deemed of special value for operational applications regardless whether such writing was formally required. This is the seventeenth report in the series since 1997. It deals with calibration of differential reflectivity, Z_{DR}.

In spring of 2004 at the meeting of Technical Advisory Committee (TAC) to the Radar Operation Center (ROC) the issue of Z_{DR} calibration was raised. I did not attend the meeting due to travel abroad hence the following is a here say rendition of post facto impressions. Which are that I was under the impression that the TAC was under the impression that no adequate consideration had been given to this matter. On the contrary I gave it considerable thought and had a scheme that worked on paper (translation: with merit but never been tested). The scheme uses existing automatic calibration circuits on the WSR-88D. Needless to say minor details (a year of effort!) had not been worked out. Suggestions at the meeting to use meteorological scatteres only increased the anxiety of the engineers. I am partly to blame for not divulging the scheming scheme. It was premature and other urgent (read: less important) chores were in the way. Moreover the date for the beginning of upgrade was on a schedule predicted by me, guessed my many, but not admitted by any, so there was ample time for development.

The procedure on how to calibrate differential reflectivity on the WSR-88D is described here in. It has been tested on the KOUN proof of concept and achieves an accuracy of about 0.1 dB. It is straight forward, requires good engineering practice, and experience in microwave measurements. To quote a yet to be recognized philosopher: "Devils and Angels are in the details; mastery is to avoid the former and find the latter". So, graduate and undergraduate students, post docs, academicians, as well as professors at esteemed to be Universities do not qualify for this chore except as kibitzers.

I thank Allen Zahrai for leading the team of engineers who designed the new processor and controls of the radar and oversaw subsequent modifications used herein. Igor Ivic gave valuable advice concerning coherent leakage. Mike Schmidt and Richard Wahkinney made extensive modifications of microwave circuitry and controls and actively participated in many measurements.

May 2005 in the prairie town of Norman where all meteorologists are No. 1 and engineers are second to none!
Dusan S. Zrnic

CALIBRATING DIFFERENTIAL REFLECTIVITY ON THE WSR-88D

National Severe Storms Laboratory Report

prepared by: Dusan S. Zrnic, Valery M. Melnikov, and John K. Carter

May 2005

NOAA, National Severe Storms Laboratory
1313 Halley Circle, Normal, Oklahoma 73069

Contents

CALIBRATING DIFFERENTIAL REFLECTIVITY ON THE WSR-88D

Introduction

On polarimetric radars which transmit simultaneous horizontal and vertical polarizations three polarimetric variables must be calibrated. These are reflectivity factor, differential reflectivity, and differential phase. Reflectivity factor remains the most difficult and elusive. Differential phase is not calibrated per se; rather the system differential phase is measured to determine the beginning of the phase unwrapping interval (Zahrai and Zrnic 1993). This can be done easily using ground clutter (Zrnic et al. 2005). Differential reflectivity does need to be calibrated and this paper suggests a way to do it on the WSR-88D network. Section 1 describes a step by step procedure. Constraints and assumptions are also listed. Section 2 contains more detailed description on how to make the measurements and presents results obtained on the KOUN polarimetric radar. Section 3 discusses an alternate method for calibrating differential reflectivity; for the proposed polarimetric WSR-88D that method has practical disadvantages. More measurements were made than listed in the steps of first section. These were done to verify the overall procedure. Sentences in italic highlight important details; whereas adhering to these does not guaranty a well calibrated Z_{DR} for operational use, skipping will result in a calibration worthy of academic discussion and presentation at PT meetings.

1. Functional description

In developing the procedure we set the following goals. 1) Use existing parts and capabilities of the current WSR-88D; this eliminates calibration at vertical incidence, or addition of extra hardware beyond at most one mechanical switch. 2) Calibration must be possible immediately after retrofitting the radar; this eliminates reliance on precipitation. 3) Calibration should be over the full dynamic range; this enlists variable attenuator. 4) There should be no temporal drift in the calibration curve between volume scans; this demands calibration at the end of each volume scan.

The block diagram in Fig. 1 captures the gist of the KOUN radar with points labeled 1 to 4 which are relevant for the subsequent discussion. The single line arrow

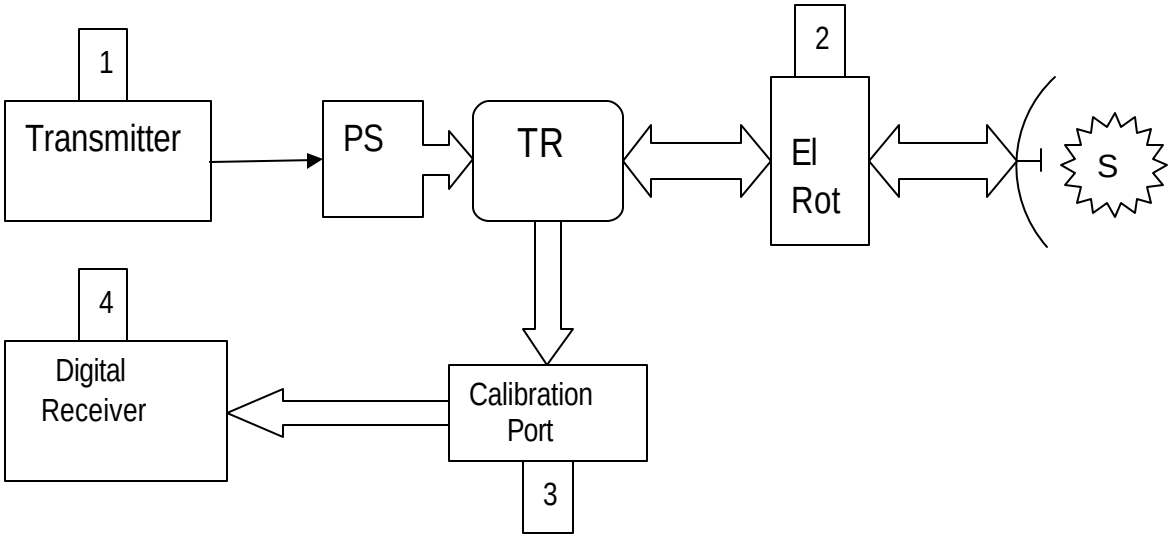

Fig. 1.1 Diagram of the KOUN system with crucial points for calibrating Z_{DR}.

connects Transmitter to the Power Splitter (PS) and corresponds to the waveguide on KOUN which goes from the transmitter to the pedestal. Block arrows indicate two channels H and V as well as direction of signal flow. The H and V signals are simultaneously transmitted and received.

Point 1 represents coupler for transmitter power measurement. Point 2 represents two couplers above the elevation rotary joints for power measurements. Point S is the sun's radiation flux at the antenna. Point 3 corresponds to calibration couplers near the input to the LNAs. Between it and LNA is a waveguide filter (bandwidth ~ 16 MHz) and receiver protector. A variable attenuator under computer control is connected to a signal generator (or noise generator) for calibrating automatically the receiver. This is standard on the WSR-88D and it is crucial for maintaining calibrated Z_{DR}. Point 4 represents output of the digital receiver, that is digital I, Q values of both H and V components; from these one computes various powers, noises, and differential reflectivity.

The premise behind the procedure is to partition calibration into parts which are constant (time invariant) and parts which can vary with time. The time invariant part is measured once to establish the constant bias valid for the full dynamic range. The slowly varying part is tracked over the full dynamic range from volume scan to volume scan analogous to the AGC calibration in the Legacy system. Initially the sun scan is used to determine the two way bias between the elevation rotary joint and the space outside the radome. There are two assumptions in the calibration procedure. First, the time constant of the slow drift is considerably longer than duration of volume scan. This is needed because measurements are sequential and some have common paths, so we assume there are no changes between measurements. This assumption must be checked by repeating the measurement. Second, the sun's radiation is randomly polarized so that the horizontal and vertical components have equal mean powers.

Bias between any two points is denoted with the symbol $?_{ij}$, where the first subscript (i) is the input point and the second is the output. Although $?_{ij} = ?_{ji}$, some of the

bias can be easily measured in one direction because of the placement of couplers, or signal flow. Hence in general the signal flow direction both during measurement and actual operation is from the port indicated by the first index.

Bias measurement procedure

1) *Transmission chain*

1.1) Point 1 to point 2:

Differential reflectivity in the transmission chain must be measured at the time of retrofit.

Deviation from 0 is the bias $?_{12}$. (1.1)

NSSL measurement indicates $?_{12} = -0.06$ dB (i.e., $10\log_{10}(P_h/P_v)$).

1.2) Point 2 to outside of radome:

This is more involved and round about because it is deduced from measurements in the receiving chain (see 2.3)).

The bias is denoted with $?_{2S}$. (1.2)

2) *Receivers' chain*

2.1) Point 3 to point 4: Split the power of the internal generator after the variable attenuator and apply to both couplers. Change attenuation in steps of 2 dB over the whole dynamic range. Generate the curve of Z_{DR} vs power P_{hk}, where P_{hk} is the value of attenuated power in the horizontal channel at the output of digital receiver and k is the setting index. This power is in units internal to the digital receiver (i.e., digital numbers which are uniquely related to the input powers at the antenna – but that relation is immaterial for computing the bias!). Ideally this Z_{DR} curve should have the value of 0 dB;

deviation is the bias $?_{34}(P_{hk})$. (1.3)

This bias is constant over most of the dynamic range of the receiver (except at saturation).

NSSL measures $?_{34} = -0.44$ dB.

Make this measurement immediately after 1.1); the value presented herein was obtained on March 10, 2005.

2.2) Point 2 to point 4: Take a signal generator, split its power and inject into the two couplers above the elevation rotary joints. Make few measurements of differential reflectivity by changing the power of the signal generator.

Record the bias $?_{24}$. (1.4)

NSSL measures $?_{24} = -0.75$ dB.

Take the difference between (1.4) and (1.3) to obtain $?_{23}$

NSSL measures (on March 10) $?_{23} = ?_{24} - ?_{34} = -0.31$ dB (1.5)

Repeat measurement 2.1) to make sure that nothing has changed. Then go to 2.3).

2.3) Point outside of radome to 4: Use sun scan and record differential reflectivity bias

$?_{S4}$. (1.6)

NSSL measures (on March 17) $?_{S4} = -0.69$ dB.

2.4) Point outside the radome to 3:
Apply the internal noise generator to the LNA inputs and measure again the $?_{34}(N_g)$. Do not use the value obtained with the CW generator, i.e., the one from 2.1)! Then measure again the $?_{34}$ with the CW generator. If the two measurements with the CW generator agree accept the measurement with the noise generator. Otherwise split the difference or repeat the measurement.

The difference $?_{S3} = ?_{S4} - ?_{34}(N_g)$ (1.7)

obtained from 2.3) and the new $?_{34}(N_g)$ is this bias.

NSSL measures (on March 17) $?_{S3} = ?_{S4} - ?_{34}(N_g) = -0.69 - (-0.44) = -0.25$ dB

2.4) Point outside the radome to 2:
The difference $?_{S2} = ?_{S3} - ?_{23}$ obtained from (1.7) and (1.5) is this bias. By reciprocity it is equal to the bias on transmission between 3 and outside, that is

$?_{S2} = ?_{2S}$ (see 1.2)). (1.8)

NSSL measures $?_{S2} = ?_{S3} - ?_{23} = -0.25 - (-0.31) = 0.06$ dB

Repeat measurement 2.1) to make sure that nothing has changed.

3) *Bias computation*

Sum all the fixed biases to obtain the constant bias:

$?_C = ?_{12} + 2?_{S2} + ?_{23} = -0.06 + 2x0.06 + -0.31 = -0.25$ dB (1.9)

Add this bias to the $?_{34}(P_{hk})$ to obtain the correction $?(P_{hk})$ for the whole dynamic range:

$?(P_{hk}) = ?_C + ?_{34}(P_{hk})$. (1.10)

NSSL measured (on March 10, 2005) an almost flat $?_{34}(P_{hk})$ which at the SNR corresponding to sun power was -0.44 dB. Hence the correction for most of the dynamic range was an additive 0.44 + 0.25 = 0.69 dB.

4) *Correction in real time*

At the end of each volume scan generate (1.3) than compute (1.8) and use it for correcting differential reflectivity. Remember noises in the H and V channels are different.

5) *Check at regular intervals.*

Check with the sun scan if the receiver maintains calibration. This could be done daily, weakly, or monthly.

2. Measurements on the KOUN

Measurements on the KOUN radar were made over a two year period. Beginning in 2002 the polarimetric processing was done on the Sigmet RVP7 receiver/processor, which is the time when we begun developing the Z_{DR} calibration procedure. At that time our verification was made using precipitation which has intrinsic differential reflectivity of zero (Melnikov et al. 2003). The RVP8 processor with a 36 MHz sampling rate was installed in the Fall of 2003. Due to difficulties associated with Open systems in development, (translation: metamorphosizing opaque but porous system) it took until mid Spring of 2004 to reach the status of the RVP7. Then in Oct of 2004 we replaced the digital receiver with the new model which has a 72 MHz sampling rate and will be standard on the operational network.

We present a more detailed explanation of steps outlined in section 1 and support these with measurements. Further we indicate which measurements are to be made at the time of retrofit, which at time of periodic checks, and which at end of volume scans. Notation and order of presentation follow section 1.

The essence in the calibration procedure is to separately measure the constant bias $?_C$ and the time varying bias $?_{34}$. Then update at the end of each volume scan the time varying part. The constant bias must be measured at the time of retrofit, and could be checked occasionally after changes on the system have been made, or during periodic maintenance.

The *fixed bias from transmission and back to the calibration port is*

$$?_C = ?_{12} + 2?_{2S} + (?_{24} - ?_{34}) \qquad (2.1)$$

where $?_{2S}$ *is the bias between the El joint (at port 2 in Fig. 1.1) and the antenna output referred to outside of radome* (Figs, 1.1 and 2.4). The factor 2 accounts for the two way path (transmit and receive). This $?_C$ is constant and will be stable because it is caused by fixed passive components. The remaining bias $?_{34}$ from calibration port (3 in Fig. 1.1) to output of digital receiver is caused by the two active receiver paths (input to the LNA, mixers, and amplifiers). Thus $?_C$ will be added to the variable bias. Unless stated otherwise the bias is expressed in dB.

2.1 Measurement of constant biases in transmission chain

2.1.1 *Point 1 to point 2,* (**?** $_{12}$)

Waveguides were opened at the elevation rotary joints (point 2, Fig 1.1). Power was injected at the coupler (point 1 in Fig 1.1) just above the transmitter. The difference at the output of the two wave guides was about 0.04 dB, for all practical purposes non discernible. At that time we measured and recorded the coupling losses; these agreed exactly with the values stamped by the manufacturer. *Because there are no reasons for the polarimetric WSR-88D radars in the network to be any different we recommend bypassing this step and making the measurements at the output of the couplers at the time of retrofit. Nonetheless, comprehensive measurements should be made on the preproduction model to back this recommendation. Differences in coupling must be accounted for.*

Next the wave guides were properly connected, the transmitter was turned on, and measurements were made at the couplers above the elevation rotary joints. Figure 2.1

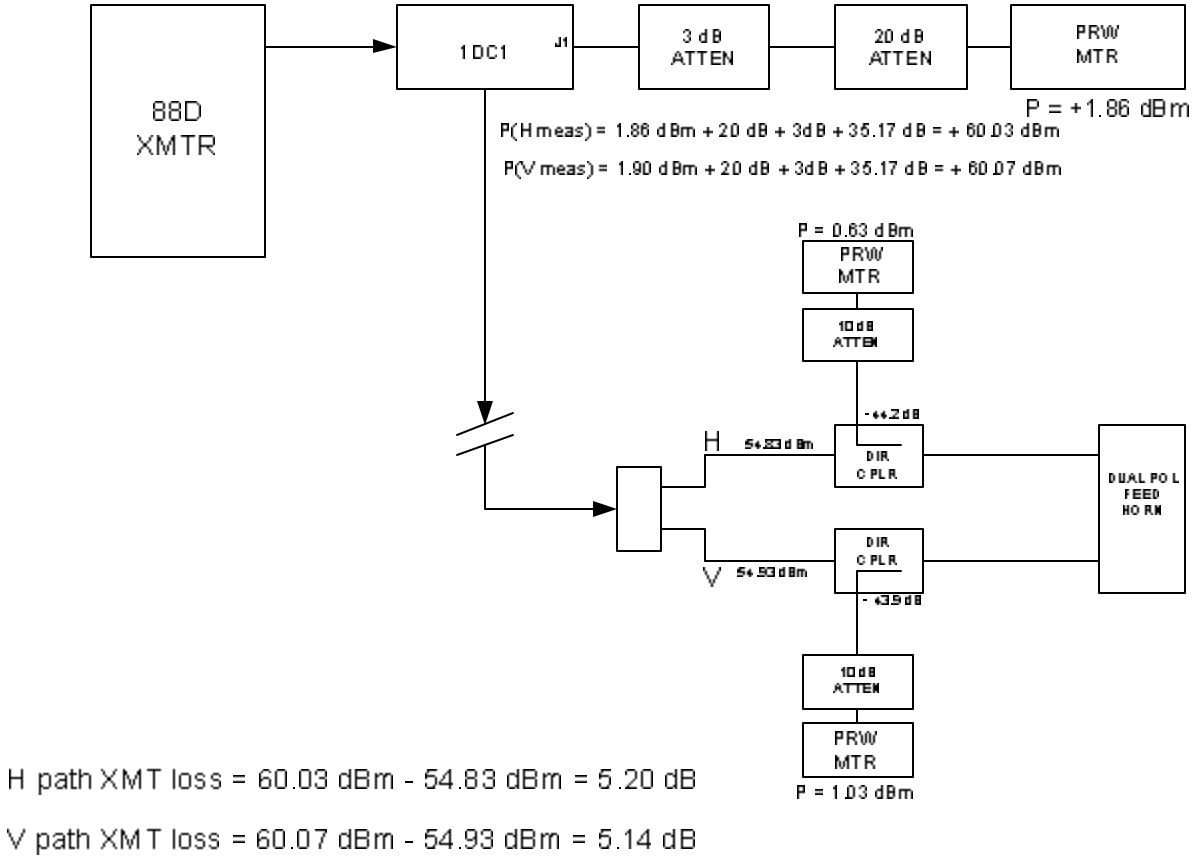

Fig. 2.1 Schematic for measurement of difference in transmitted powers; measured values are indicated. 1DC1 and J1 are points depicted in the WSR-88D drawings.

illustrates the paths and values of power levels. For safety it may be wise to reduce the transmitter power by 10 or 20 dB, which we have not done on the KOUN!

Because the measurements were made sequentially we have recorded the transmitter power during each measurement (values are in Fig. 2.1). This is highly recommended!

In Figure 2.1 the P(H meas) signifies the input power inside the guide in dBm; it consists of the one read off the meter (1.86 dBm) plus two attenuators (3 and 20 dB) plus the loss through the coupler (35.17 dB). Similarly the P(V meas) is computed (the meter showed 1.9 dBm). The coupler losses (at the elevation rotary joints) and attenuator settings at the power meter inputs are indicated. The measured power loss in the H path is 5.2 dB and in the V path it is 5.14 dB. The difference of losses between the H and V channels is 0.06 dB (H higher), in excellent agreement with the measurement on open waveguides. Thus we record $?_{12}$ = -0.06 dB.

Before the change to dual polarization the loss in the H channel (according to adaptation data) was 1.52 dB. Adding 3 dB of power lost via the splitter brings the total to 4.52. Therefore the change to dual polarization on KOUN has increased loss by (5.2 - 4.52) = 0.68 dB. There should be no such increase in the production model of the dual polarization WSR-88D. On the KOUN the microwave components are assembled outside the pedestal with the primary requirement for easy access to accommodate changes and measurements. This will not be the case on the production units.

From the coupler above the elevation joints to the feed horn the specified loss (but not measured) is 0.2 dB and therefore the match between the two channels in the transmit chain up to the feed horn is considered to be perfect. Nonetheless there could be a differential gain of the antenna at two polarizations. Measurement from sun scan will establish this.

2.1.2 ***Recommendation for measurement at the time of installation of the dual polarization system***

1. *Coupling loss in waveguide couplers above the elevation rotary joints.*

Normally these are measured by the manufacturer and stamped with the value. *If not, it is imperative to make this measurement as these couplers affect both receiver and transmitter calibration.*

2. *Difference in power between transmitting channels at the couplers above the elevation joints.*

Stop antenna and point high and away from the sun. Turn transmitter on. Measure powers at the outputs of the elevation rotary joints (point 2, Fig. 1.1).

Use one power meter for both measurements and repeat the measurement to make sure results are consistent. Take into account the coupling differences between the two couplers.

The difference in powers is the bias $?_{12}$.

2.2 Measurements of constant bias in receiving chain

2.2.1 Receiver noise levels in the two channels

This is straight forward. It requires antenna to be pointed high into the sky away from the ground. The two noise powers N_h and N_v should be recorded. On the KOUN the N_h = -113 dBm and N_v=-114 dBm. (We recommend that in future upgrade the noise powers at each elevation angle be measured either from regions of no echo, or from spectral analysis, ideally noise power should estimated for each radial.) We offer Fig.

2.2, to alert readers about variability of noise due to interference which at KOUN has strong spatial dependence. *For calibration of Z_{DR} it is imperative to avoid erratic noise and interference.*

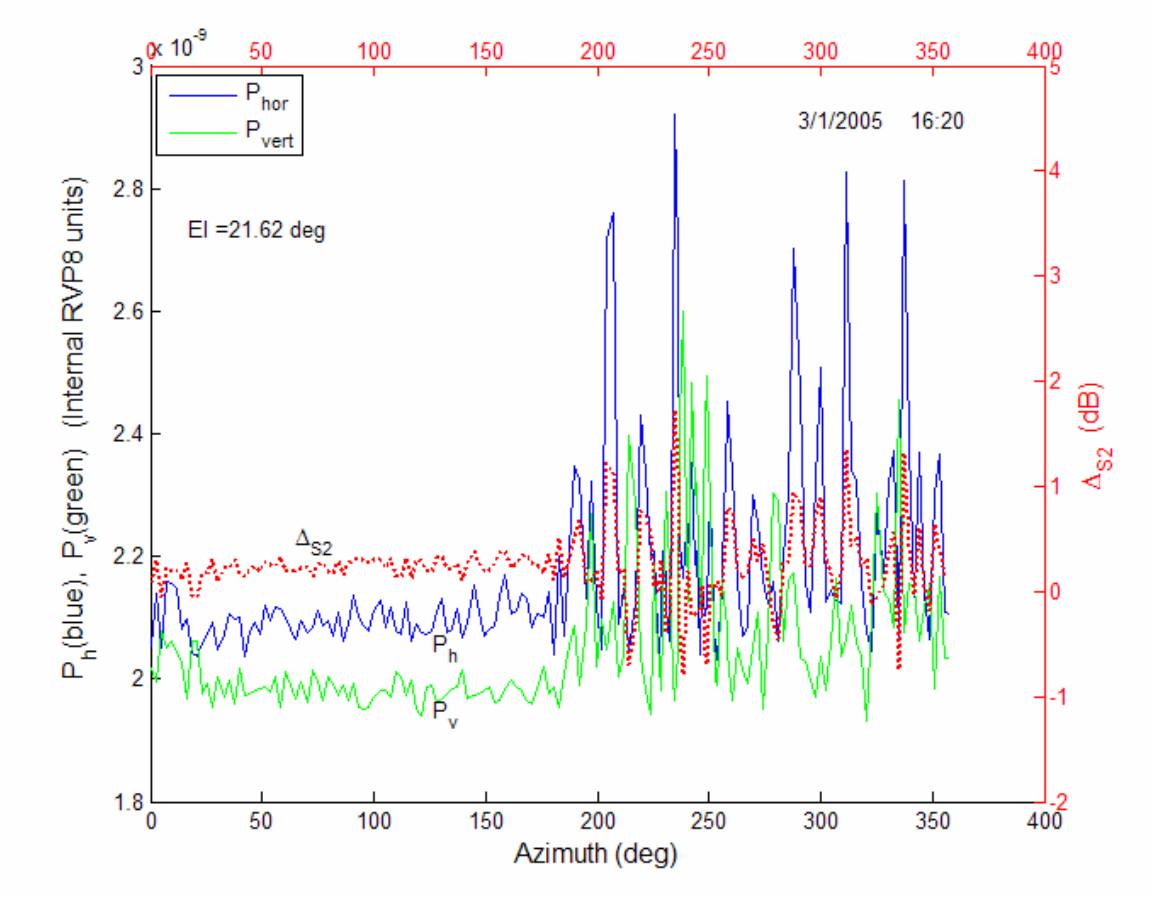

Fig. 2.2. Receiver noise powers (in internal *linear* RVP8 units) and differential reflectivity (dotted curve) as function of azimuth on the KOUN radar. The relatively constant noise in the vertical channel between 20 and 170 deg corresponds to -114 dBm at the LNA input. The noise in the horizontal channel corresponds to – 113 dBm.

2.2.2 Difference in receiver chain from El couplers to input of digital receivers

This measurement is for consistency and can be bypassed because the next one (section 2.3.3) encompasses its path. Nonetheless it might be convenient in case of trouble shooting.

Turn transmitter off. Use signal generator and set it to - 20 dBm power, split its output, *compare the split powers and record the difference (we measured -0.07 dB)* for precise determination of bias. Inject the split signals into the couplers above the elevation rotary joints. A good range of generator power for this measurement is between -30 dBm to 10 dBm. Above this range saturation effects might appear and below this range receiver noise begins to affect the measurement. Measure the powers at the output of the IF amplifiers in the H and V receiver channels. Take the difference in dB and *correct for cable and coupler differences (on KOUN add 0.34+0.07)* co compute the bias in Z_{DR} up to that point.

The measurement schematic for KOUN and results are depicted in Fig. 2.3. Gain in the H channel is smaller by 0.12 dB from the gain in the V channel. This again is a negative bias of -0.12 dB.

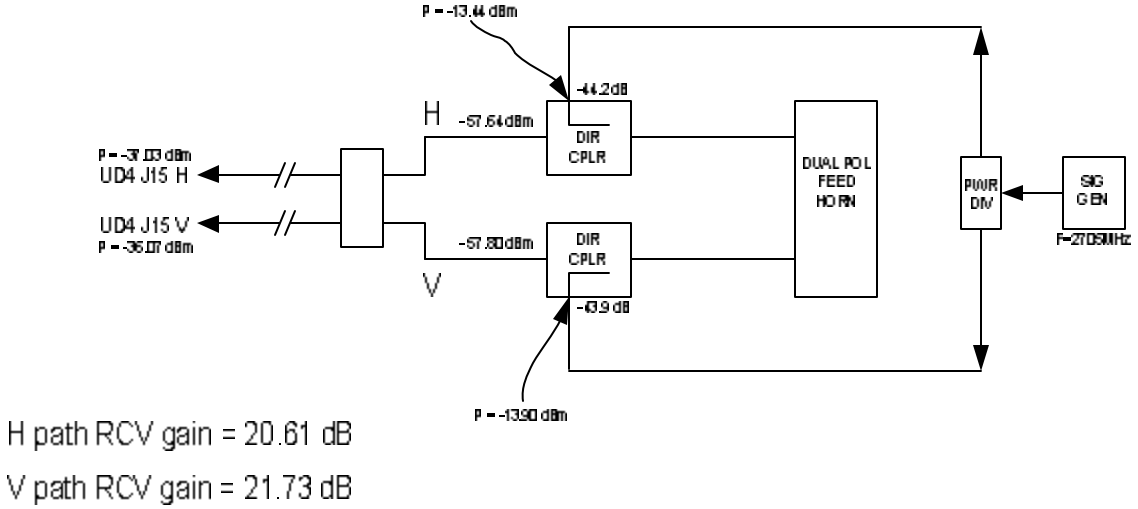

Fig. 2.3. Schematic for measurement of difference in Z_{DR} from couplers above El joints to the input of the digital receivers.

2.2.3 Difference in receiver chain from El couplers to the calibration port (? 23)

Two measurements are recommended to obtain **? 23**. These are measurement of **? 24** and measurement of **? 34**, so that

$$?_{23} = ?_{24} - ?_{34} \text{ is the difference bias.} \qquad (2.2)$$

Both are described in the sequel.

2.2.3.1 *Difference from El coupler to the output of digital receiver* (**?** $_{24}$).

The sole purpose of this measurement is to combine it with the one between the calibration port and digital receiver output (2.3.3) so that the fixed bias from El coupler to the calibration port can be computed (Fig. 1.1 and 2.4). This measurement should be done in real time with the signal processor; on the KOUN we recorded time series data to obtain the values.

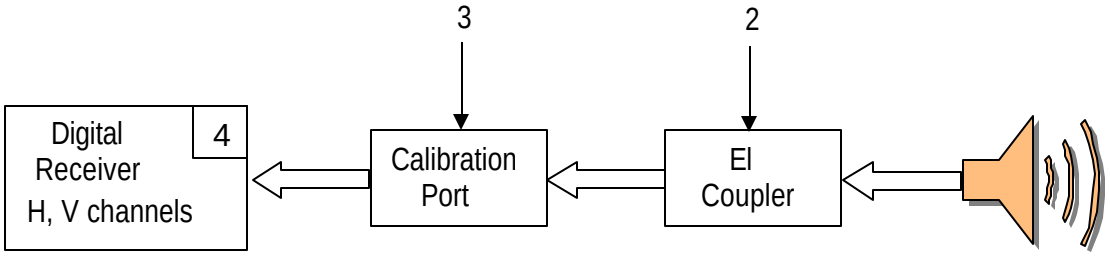

Fig. 2.4 Schematic for calibrating the receiver chain.

Inject a CW signal (HP generator) at the coupler above elevation rotary joint (as in 2.2.2, port 2 in Figs. 1.1 and 2.4) and measure the powers from H and V channels at the output of the digital receiver (i.e., I, Q powers). A good value for the signal power is about – 20 dBm which amounts to (-20 - Insertion Loss - 3) dBm – *referred to the power in the waveguide at the elevation rotary joint*. Insertion Loss is about 44 dB (but different for the two channels, see exact values in Fig. 2.3) so that the power would correspond to about –67 dBm of weather signal or an SNR of over 45 dB. Hence the effect of receiver noise is negligible on determination of this bias. *Make sure that the SNR = 30 dB so that the receiver noises have no effect on the measurement.*

Now decrease the power in 3 dB steps to about -32 dBm. Record the values of bias $\Delta_{24}(P_j)$ where P_j are few powers at the output of digital receiver. *These are in arbitrary units! For Z_{DR} calibration no absolute value of power is needed, but the changes in relative values of power at the digital receiver output must be known. Average the values if they change by less than 0.05 dB.* Over a range of 50 dB this bias on the KOUN changes by less than 0.05 dB (see Fig. 2.5).

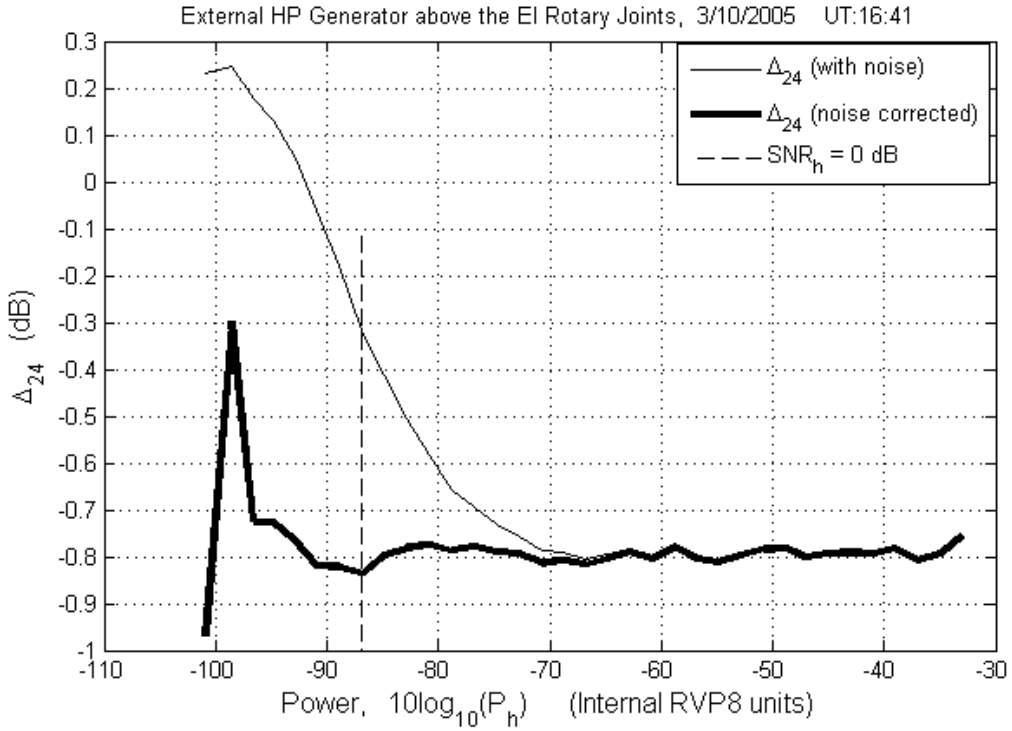

Fig. 2.5 Bias Δ_{24} measured on the KOUN. The dashed line indicates receiver noise power (in internal relative RVP8 units).

In Fig. 2.5 is the $\Delta_{24}(P_j)$ obtained on the KOUN over a much larger dynamic range than needed for this calibration. It suffices to choose a 10 dB interval in the middle of dynamic range (somewhere between -40 and -60 dB in Fig. 2.5). The $SNR_h = 0$ dB corresponds to – 113 dBm referred to the LNA input. The P_h on the ordinate is the output power from which the noise power N_h has been subtracted, i.e., $P_h = P_{htotal} - N_h$. Two bias curves are shown; in one the noises N_h and N_v have been subtracted from P_h and P_v to compute the bias, in the other they have not. This is to illustrate the match between the

two channels, and to determine the value at which receiver noises begins to influence the measurement. Note the difference between Ψ_{24} (-0.75 dB) measured on March 17 (see page 4) and -0.8 measured on March 10 (Fig. 2.5). *In this and all other plots and measurements the differences in coupling losses have been accounted!*

For calibration at the time of retrofit the output powers should be at least 30 dB larger than receiver noise. Then noise effects can be ignored to speed up this manual measurement.

2.2.3.2 *Calibration port to output of digital receiver* (Ψ_{34})

This calibration can be done as described in section 2.3.1 but should be automated. On the KOUN we have done it manually. *Only values at strong SNR are used for fixed bias computation!*

Connect the internal CW generator to the calibration ports of the H and V receivers (port 3 in Fig. 2.4; this features is automatic and internally build in the WSR-88D for the H channel). For the polarimetric WSR-88D a hardware modification is required to include addition of power splitter. *Check the power using the internal generator. Apply the internal generator (set internal attenuator to about 40 dB) through the splitter to the two LNAs and record the difference between the two outputs (on the KOUN the H output is higher by 0.04 dB). Record the difference between the two couplers using stamped values by the manufacturer (on KOUN this difference is 0 dB)! The total difference between the couplers and in power splitting is constant and must be accounted in all measurements with the internal generators.*

Plot the bias curve $\Psi_{34}(P_k)$ as suggested in section 2.3.1.2 Look at the bias for the range of power values which overlaps the P_j in $\Psi_{24}(P_j)$ from measurement described in section 2.2.3.1.

The difference in the overlapped part between the two curves $\Psi_{24} - \Psi_{34}$ is a constant bias Ψ_{23}, independent of P_j. A good estimate is obtained by averaging the ratios (bias in linear units) or by averaging the bias in dB units in the region of overlapping P_j. This bias is introduced in the receiver between the Calibration port (3 in Fig. 2.4) and the port above the Elevation joint (2 in Fig. 2.4). In these parts of channels there are no active components hence the bias will be fixed.

Make the measurements of Ψ_{24} and Ψ_{34} in rapid succession to avoid possible drifts in receiver gains between the measurements. That is first Ψ_{34} then Ψ_{24} then Ψ_{34}; if Ψ_{34} does not change between measurements the bias (eq. 2.2) is valid. If it changes scratch your head and start over. Or split the difference if it is less than 0.06 dB.

2.2.4 Difference from the outside of radome to El couplers (Ψ_{S2})

Like 2.2.3 this measurement requires two steps and use of previously determined value of Ψ_{23}. The equation is

$$\Psi_{S2} = \Psi_{S4} - \Psi_{34}(N_g) - \Psi_{23} . \qquad (2.3)$$

Note, Ψ_{S4} is measured with the sun scan, and $\Psi_{34}(N_g)$ must be measured with the internal noise generator!

To distinguish the Ψ_{34} measured with internal noise generator we have included (Ng) in parenthesis. There are two reasons why the noise generator must be used: 1) The sun, noise generator and the weather signal are broad band whereas the signal generator

is narrow band. The two receivers might not be identical, there is the obvious difference of gains which can be calibrated with the narrowband CW generator; but the small difference of integrated powers (over all frequencies) of broad band signals could be of the order of 0.1 dB (on KOUN it is less than quantization of 0.06 dB inherent to the Sigmet A-scope). 2) On the KOUN there are leakage signals if the internal CW generator is connected and these affect measurements at SNR < 30 dB. No leakage signals are present if the internal noise generator is connected. Furthermore, in the differential measurements with the noise generator and the sun, the difference between the frequency transfer functions of the two receivers cancels out (see Appendix A).

In the case of KOUN the values of Ψ_{34} obtained with the internal noise generator are lower from the values obtained with *internal signal generator* (at SNRs < 30 dB) due to coherent lekadge. The difference is repeatable, although the absolute bias in differential reflectivity slowly changes. There is no such difference if amplified noise and strong signal from the internal CW generator (> 40 dB SNR, the output from the internal noise generator is amplified to obtain sufficient power) are used.

2.2.4.1 *Calibration port to output of digital receiver* $\Psi_{34}(N_g)$ - *internal noise generator*

As explained in section 2.2.4, Ψ_{34} must be measured again. To make the measurement use the internal noise generator and build in attenuator in the range from 0 to 20 dB; this results in an output signal (from the noise generator) to receiver noise ratio of 22 to 2 dB. To measure the N_h and N_v increase attenuation to a large value (> 60 dB).

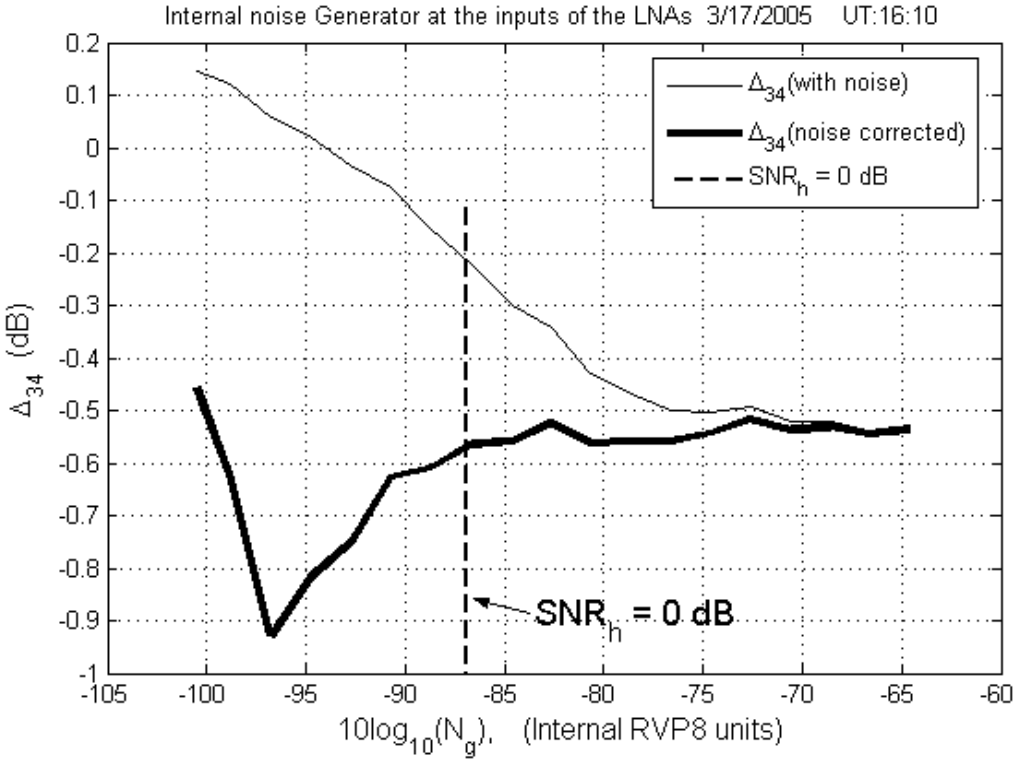

Fig. 2.6 Bias in differential reflectivity Ψ_{34} measured with the internal noise generator. The receiver noise level N_h (subtracted from P_{htotal}) would correspond to -86.8 units.

That way the noise generator need not be disconnected as it would have no effect on the measurement. Make sure there are no outside interferences. Compute $?_{34}(Ng_{hk})$, where Ng_{hk} stands for the power at the output of digital receiver *after subtraction of noise power* N_h (internal RVP8 units), h stands for the horizontal channel, and k is attenuator index (number of points for measurement). The $?_{34}(Ng_{hk})$ measured on the KOUN is plotted in Fig. 2.6. For the noise corrected curve the receiver noise powers were subtracted before computation but in either case the noise generator power on the abscissa $N_g = P_{htotal} - N_h$, where P_{htotal} is the estimate at the output of digital receiver and N_h is the receiver noise power estimate (also at output of digital receiver).

The noise corrected bias (Fig. 2.6) is fairly uniform down to the $SNR_h = 0$ dB. The change thereafter is due to small coherent leakage and noise. Because the power from the sun is typically between -75 and -80 units, the measurement (on the KOUN) is sensitive to these effects. We expect the same to hold on the polarimetric WSR-88Ds.

2.2.4.2 *Sun scan for* $?_{S4}$

Determine the powers from the sun in the horizontal channel and in the vertical channel; subtract the corresponding noises from these powers and compute the value of differential reflectivity. Thus $?_{S4}$ will be measured at only one value of power.
The procedure used with the RVP7 processor is documented in Melnikov et al. 2003 (page 31). We used it with the RVP8 as well; only this time the two receiver bandwidths are much better matched so that the measurement is more precise. Briefly we scan the

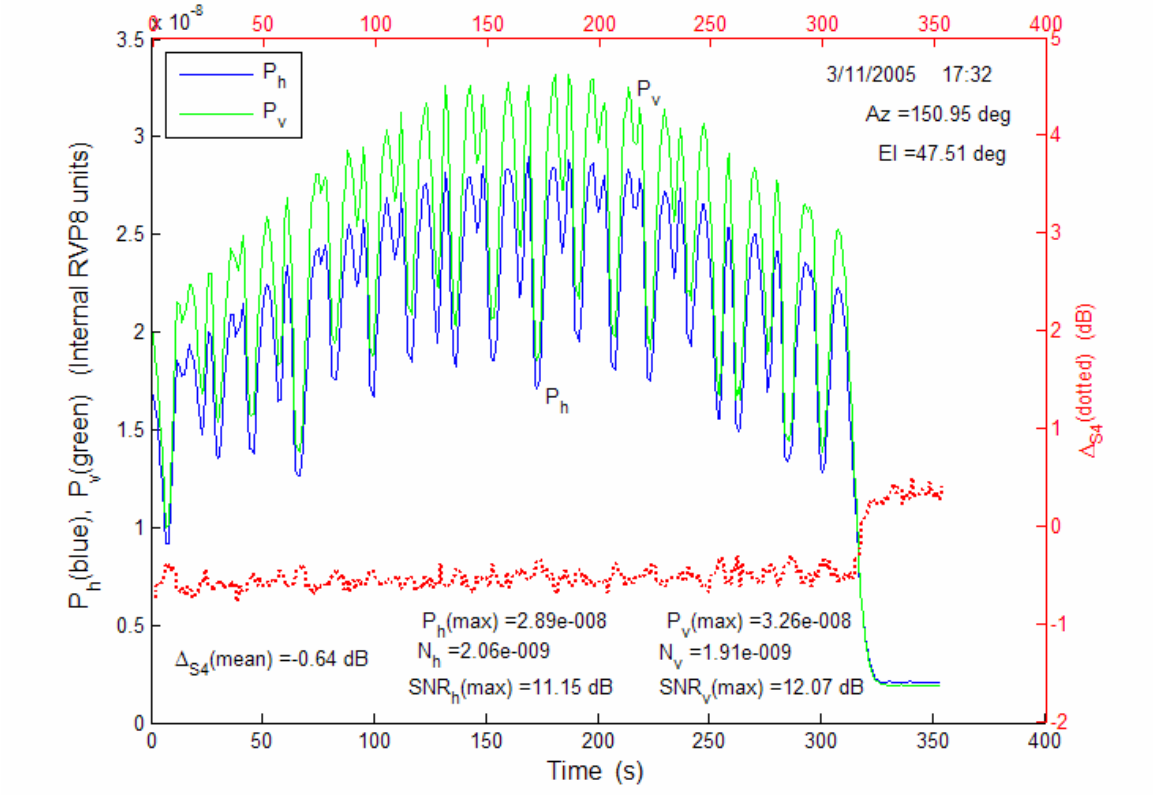

Fig. 2.7 Sun scan. Powers at horizontal and vertical polarizations (linear internal RVP8 units) and bias in differential reflectivity $?_{S4}$.

antenna over a small sector at an elevation close to the elevation of the sun. We let the sun drift through the scanning plane and record $?_{S4}$ (that is Z_{DR}) and P_h (see Fig. 2.7). The peak of P_h indicates that the sun is centered on the beam. There will be several peaks (Fig. 2.7) as the sun enters the plane of the scan. The highest of the peaks is identified and differential reflectivity is computed for that point and all the points up to 2 dB below it. The average of these values is the differential reflectivity bias $?_{S4}$.

Noises N_h and N_v must be subtracted before computing the differential reflectivities. These noises are estimated at the end of sun scan.

Plotted in Fig. 2.7 are P_h and P_v (in linear units at the output of digital receiver) and differential reflectivity $?_{S4}$ (dotted curve). The noises N_h and N_v have not been subtracted in any of these plots. One can see that the bias is near -0.6 dB. At the time of about 310s there is a sharp increase of differential reflectivity and drop in signal powers. This is when we begun receiver noise measurement. Clearly the difference in noise powers between the two receivers causes discontinuity in differential reflectivity. In the KOUN case the SNR from the sun scan is typically 10 dB.

To give readers a feel of the stability of the measured differential reflectivity from the sun (noise corrected), we list values obtained over about 1 hour of time on March 11, 2005 (same day as for data in Fig. 2.7). Noises have been subtracted to compute $?_{S4}$. The rms deviation about the mean (~ -0.62 dB) of these measurements is 0.025 dB.

Table 1: $?_{S4}$ measured on March 11, 2005 over a period of one hour

Time (CST)	16:51	17:03	17:012	17:21	17:32	17:42
$?_{S4}$ (dB)	-0.59	-0.66	-0.64	-0.64	-0.64	-0.60

The estimated values of $?_{S4}$ and $?_{34}(N_g=P_{sun})$ are substituted into (2.3) to obtain the bias $?_{S2}$. Because the $?_{34}(N_g)$ is available in discrete increments one might need to interpolate to obtain the $?_{34}(N_g=P_{sun})$ at the power corresponding to the power from the sun.

Next, in Table 2, we present $?_{34}(N_g)$, $?_{S4}$, and their difference measured over several days. The sun scan measurement was preceded with the "before" and followed

Table 2: Measurement of $?_{S4}$, and $?_{34}$ over several days

Date	Time	$?_{34}$ Noise Gen before (dB)	$?_{S4}$ Sun scan (dB)	$?_{34}$ Noise Gen after (dB)	$?_{S3} = ?_{S4} - ?_{34}$ (dB)
03/17/2005	15:46	-0.50	-0.76	-0.50	-0.26
	16:18	-0.50	-0.79	-0.50	-0.29
	17:01	-0.50	-0.82	-0.50	-0.32
	17:43	-0.50	-0.83	-0.50	-0.33
03/21/2005	15:30	-0.31	-0.60	-0.31	-0.29
03/25/2005	15:21	-0.19	-0.48	-0.19	-0.29
03/29/2005	14:52	-0.25	-0.51	-0.25	-0.26
03/31/2005	15:41	-0.42	-0.73	-0.50	-0.31 or -0.23
	15:50	-0.50	-0.74	-0.42	-0.24 or -0.31

	16:00	-0.42	-0.72	-0.42	-0.30
	16:10	-0.42	-0.72	-0.42	-0.30
	16:20	-0.42	-0.68	-0.42	-0.26
	16:32	-0.42	-0.69	-0.42	-0.27
	16:45	-0.42	-0.69	-0.42	-0.27
04/01/2005	13:56	-0.38	-0.68	-0.38	-0.30
04/04/2005	13:59	-0.31	-0.58	-0.31	-0.27
04/08/2005	14:40	-0.31	-0.61	-0.31	-0.30
	14:50	-0.31	-0.64	-0.31	-0.33
04/11/2005	21:20	-0.54	-0.84	-0.54	-0.30
04/14/2005	14:49	-0.25	-0.54	-0.25	-0.29
04/27/2005	13:54	-0.38	-0.64	-0.38	-0.26
05/06/2005	13:29	-0.25	-0.58	-0.25	-0.33
05/11/2005	13:31	-0.54	-0.88	-0.54	-0.34
05/20/2005	13:12	-0.25	-0.54	-0.25	-0.29
06/01/2005	13:36	1.20	0.87	1.20	-0.33
06/03/2005	13:09	0.64	0.31	0.64	-0.33
07/06/2005	12:59	1.60	1.24	1.60	-0.36
	13:11	1.58	1.24	1.60	-0.34
07/08/2005	13:15	1.58	1.26	1.58	-0.32
	13:25	1.58	1.25	1.58	-0.33
	13:35	1.58	1.22	1.58	-0.36
07/13/2005	14:15	1.51	1.20	1.51	-0.31
	14:36	1.51	1.21	1.51	-0.30
07/15/2005	13:38	1.58	1.25	1.58	-0.33
	13:53	1.51	1.19	1.51	-0.32
07/18/2005	13:48	1.51	1.21	1.51	-0.30
	13:57	1.51	1.19	1.51	-0.32

Mean $?_{S3}$ = -0.30 dB, standard deviation = 0.028 dB.

by "after" measurement using the Noise generator. The time between the two measurements with the noise generator was about 10 min. Note the remarkable stability of the difference $?_{S4} - ?_{34}$. In all but two cases there were no changes in the before and after measurements; until June 15 we had to manually disconnect the cables between ports to make the measurements, thereafter we used a mechanical switch. The 0.028 dB standard deviation might be caused by variations in the polarization of sun's radiation.

Measure $?_{34}(N_g)$ *and* $?_{S4}$ *in rapid succession to avoid possible drifts in receiver gains between the measurements. That is, first* $?_{34}(N_g)$ *then* $?_{S4}$ *then* $?_{34}(N_g)$*; if* $?_{34}(N_g)$ *does not change accept* $?_{S4}$ *and use it in (2.3), if not read page 11.*

Calibration with the sun scan must be made at the time of retrofit. The measurement should be repeated if changes are made above the LNAs in the receiver chain. Noise powers at the output of digital receiver (arbitrary units) N_h *and* N_v *should be subtracted. The measurement is also recommended at regular (longest) intervals scheduled for the reflectivity calibration.*

2.3 Calibration over the full dynamic range

The active receiver paths should be calibrated over the full dynamic range of the receiver (i.e., for the full range of H powers P_{hk} measured at the digital receiver output) at the end of each volume scan. This way the $?_{34}(P_{hk})$ will be measured; $?_C$ will be added to it such that

$$?(P_{hk}) = ?_C + ?_{34}(P_{hk}). \quad (2.4)$$

Note: The P_{hk} in the *argument* of $?_{34}$ in (2.4) is always

$$P_{hk} = P_{hk,total} - N_h, \quad (2.5)$$

that is, the noise is subtracted from the power at the output of the digital receiver!

Thus as stated at the beginning of section 2, the total bias consists of two parts, long term stable $?_C$ and the slowly changing part $?_{34}(P_{hk})$ mainly due to the difference in the amplifiers of the two channels. This measurement should be automated.

2.3.1 Calibration with the internal CW generator

The internal signal generator's output should be split and left permanently connected to the two ports below the Az rotary joint; this was done on the KOUN. Further we have semi automated the procedure on the RRDA to step automatically through all setting of the attenuator. No such automation is yet available on the Sigmet RVP8 receiver which is passively connected to the system. Because the RVP8 will be used on the future dual pol WSR-88D we present measurements made on that system in Fig. 2.8 and 2.9.

2.3.1.1 Power

Although our primary goal is calibration of differential reflectivity we digress here to present power measurement. In Fig. 2.8 two power calibration curves (blue solid and green dotted) are displayed vs the setting of the built in attenuator. The blue one is for the horizontal channel P_h and the green is P_v; the dB values are in internal, RVP8 units.

The powers are shown at high attenuator setting (but measurements were made over the full dynamic range). The attenuator was commended via the Legacy RDA SOT; the values were changed in steps of 2 dB. Estimates of power were obtained from 128 consecutive samples (at a PRF=1013Hz), 100 range gates were used and 30 records were averages, so that the total number of samples for a power estimates was M= 128*100*30. At high SNRs (> 10 dB) this is way too many samples, but it was used throughout the calibration process to simplify the manual implementation.

The value of -87 dB (on the ordinate) corresponds to -113 dBm (SNR_h = 0 dB) which is the power of N_h. Observe that the two power curves approach asymptotes that are larger than the receiver noise power N_h (or N_v not shown). This is because the internal CW generator adds its own noise! The two curves cross because the N_h ? N_v.

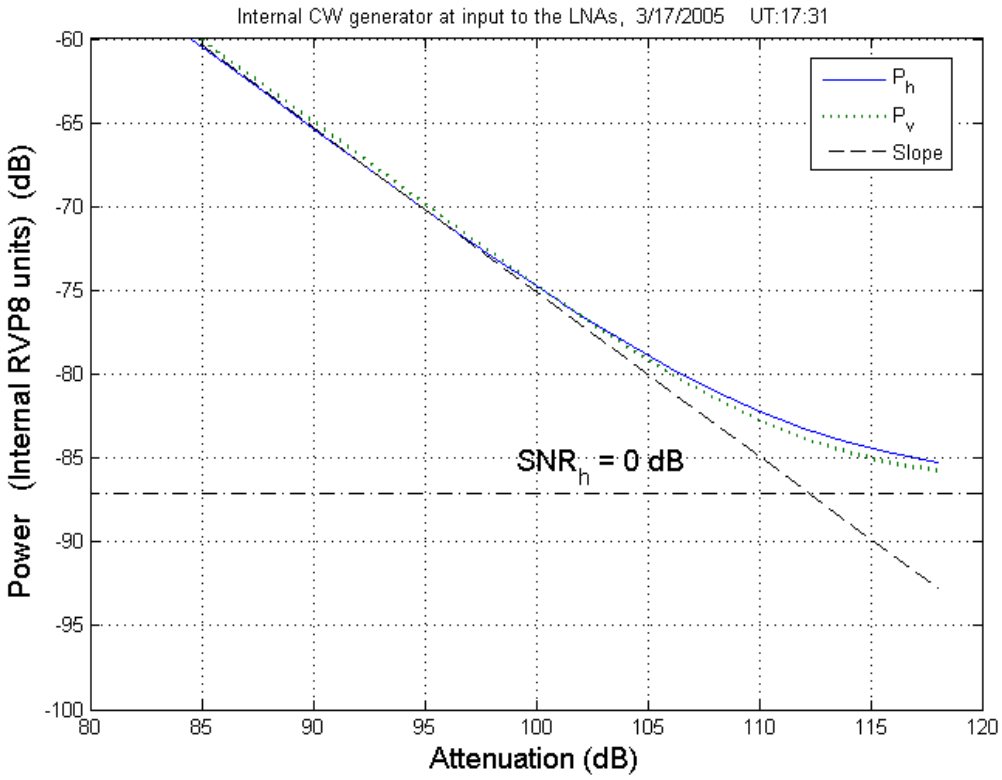

Fig. 2.8. Powers P_h and P_v at the output of digital receiver vs the setting of internal attenuator. The output power corresponding to receiver noise (i.e., SNR_h=0, -87 dB in internal RVP8 units) is indicated with the dash-dot line and receiver noises have not been subtracted from these powers.

Recommendation:

Because calibration of differential reflectivity is needed over the receivers' full dynamic range we recommend that reflectivity be calibrated at the same time. Therefore step the attenuator and record the two power transfer curves. Start with small steps (2 to 3 dB) at the high end of dynamic range (saturation range). Below 15 dB of attenuation the steps can be 5 dB down to about 55 dB. Least square fit the P_h in its linear part (from 15 dB of attenuation to about 55 dB, SNR~30 dB), project it into the weak signal region (dashed line in Fig. 2.8) and use as a transfer characteristic. For computing reflectivity factor (Z_h) use $P_h - N_h$ along the line at SNR < 25 dB. *The noise power should be measured as in 2.2.1 (generator off, receiver hooked to the antenna so that the generator noise power is eliminated from the calibration!).* Noise powers have not been subtracted in Fig. 2.8! At high attenuator settings (starting at 70 dB) a coherent leakage begins to affect the measurement; this is discussed in section 2.3.3.

Note: In the automatic calibration between volume scans (section 2.3.2) there is a constraint in step size. Too small a size would increase the time to accomplish the calibration. Maximum allowed time equals the amount of time it takes the antenna to descend from the top of volume scan to the beginning of next scan (see section 2.3.2).

2.3.1.2 Differential reflectivity

In general the number of samples to achieve a desirable error in Z_{DR} depends on the signal to noise ratio; recommendations for an automatic procedure are in section 2.3.2.

The bias curve $?_{34}(P_{hk})$ in Fig. 2.9 is computed as

$$?_{34}(P_{hk}) = 10\log_{10}\{(P_{hk,total} - N_h)/(P_{vk,total} - N_v)\}, \qquad (2.5)$$

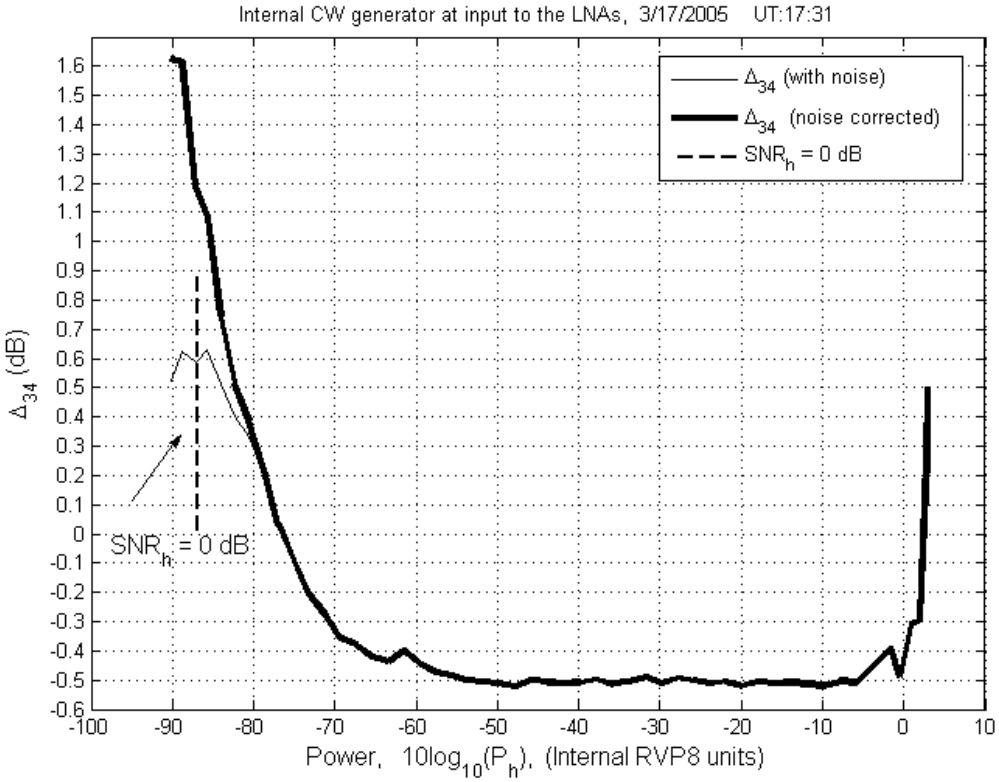

Fig. 2.9. Bias $?_{34}$ measured with the internal CW generator over the full dynamic range. The 0.04 dB difference in cables has been subtracted from (2.5) for this (and other) plots.

where the index k refers to the sequence of output power changes (corresponding to 2 dB attenuation steps), h and v refer to the polarization channels in the digital receiver, and the signal and noise powers should be estimated from numerous samples (see 2.3.2).

The units of powers on the left side of (2.5) are internal to the RVP8. Two curves are shown, the noise corrected one (as in 2.5, which supposedly should be applicable) and the curve for which the noise has not been subtracted in the right side of eq (2.5); in both cases noise N_h *is not present* in the argument of $?_{34}$. Unfortunately there is no much difference between the two curves at low SNRs. Moreover the correction is in a wrong direction. We have determined that the cause is coherent leakage.

At the high end of dynamic range the departure from the constant value is due to saturation effects. Otherwise the curve is flat down to about -55 dB. From there on the departure above the constant value is caused by the coherent leakage. This we have established by measuring with an external generator (Fig. 2.5) and with the internal noise generator (Fig. 2.6). Maximum variation in the flat part is about 0.02 dB. Recommended attenuation steps for this calibration are as in section 2.3.1.1. The reflectivity and differential reflectivity calibration should be made at the same time.

2.3.2 Automating the procedure - number of samples

Automating calibration over the dynamic range is needed for adjustment between volume scans to compensate drifts with time scales larger than volume updates. The following suggestion should be followed if the gain difference between the two channels is not constant. Measurements on more than one system are required to determine if such mismatch occurs. Otherwise follow the procedure described in sections 2.3.1.1 and 2.3.1.2.

In either case this calibration is at the end of each volume scan; it proceeds by incrementing attenuation settings and is similar to AGC scheme done on the Legacy system. At low SNR the noise power dictates the required number of samples to achieve a desired accuracy in Z_{DR}. At high SNRs very few samples are needed because the signal is a perfect sinusoid. Because of time constraint we recommend to use a variable number of samples M such that it satisfies the accuracy requirement at each calibration point. It can be shown that the required number of samples in the region of signal to noise ratios 1 to 10 (linear units) is

$$M > 200/(\text{snr}\, e)^2, \qquad (2.6)$$

where snr is signal to noise ratio in linear units and e is error of differential reflectivity expresses in dB.

At values of snr < 1 the differential reflectivity mainly depends on the receiver noise so that snr = 1 can be substituted in (2.6). To keep overall (composite) calibration of Z_{DR} within 0.1 dB let the acceptable error in measurement in Fig. 2.9 be, e = 0.03 dB. Then at snr = 1, M = 222200; with the PRF = 1013 Hz and range gate spacing of 1.16667 μs there are 592 sample I, Qs along a radial. Therefore, 222200/592 = 376 radials, or 0.37 s of dwell time are needed for computing the bias at one point. Table 2 lists some possible steps and number of radials, M_r for calibrating Z_{DR}.

Table 3: Number of radial M_r for accurate measurement of Z_{DR}

SNR (dB)	-15	-12	-9	-6	-3	0	3	6	9	12	15	18
M_r	376	376	376	376	376	376	94	24	6	2	1	1..

Adding 50 points (equivalent to 50 radials) above 15 dB of SNR for calibration (say in steps of 2 dB, to make 100 dB dynamic range) we compute $SM_r+50 = 2432$. Then with the PRF =1015 Hz we find the total time for calibration 2432/1015 = 2.4 s, which can easily be done automatically between volume scans. On the KOUN the step size of 5 dB is quite sufficient hence if the same holds on the rest of WSR-88Ds the time will be about one second.

Thus calibration should proceed as follows. Step attenuator in 2 dB increments down to 14 dB of attenuation. Then increase the steps to 5 dB and proceed until you reach 15 dB SNR. Compute the powers by averaging over M_g = 592 range gates. That is for the attenuation set at a_k find

$$P(k) = \sum_{i=1}^{M_g} [I_i^2(k) + Q_i^2(k)] / M_g \qquad (2.7)$$

The system noise power N_h is measured separately also at the end of each volume scan and should be subtracted from (2.7) (at lower SNR starting with 30 dB). Then at SNR of 12 dB and below use the number of radials from the table. If finer resolution is needed, recompute M_r. Further, if for some reason a different PRF is used, the set up for measurement would change but the total number of samples for each estimate would not.

We repeat, the outlined number of steps is for a hypothetical system which has a nonlinear gain transfer function; for systems similar to KOUN the number of steps can be much smaller and that would decrease calibration time! Further, on the KOUN the bias can be computed with larger steps of attenuation (5dB) at strong SNRs and then extrapolated from about 30 dB of SNR down to below the noise level.

2.3.3 Existing calibration circuits on the WSR-88D

For calibrating reflectivity and instantaneous gains and phases of the automatic gain control the WSR-88D has a circuit as in Fig. 2.10. The built in variable attenuator can be changed in steps of 1 dB over 103 dB of attenuation. Under computer control it connects to one of the four sources (Fig. 2.10). After the attenuator the signal is directed by a switch to either the input of the LNA or the input to the first mixer. On the KOUN the path to the LNA is split into two because there are two channels. In the Legacy calibration modes the attenuation setting is never more than 60 dB. Therefore the coherent leakage that we experience was never detrimental.

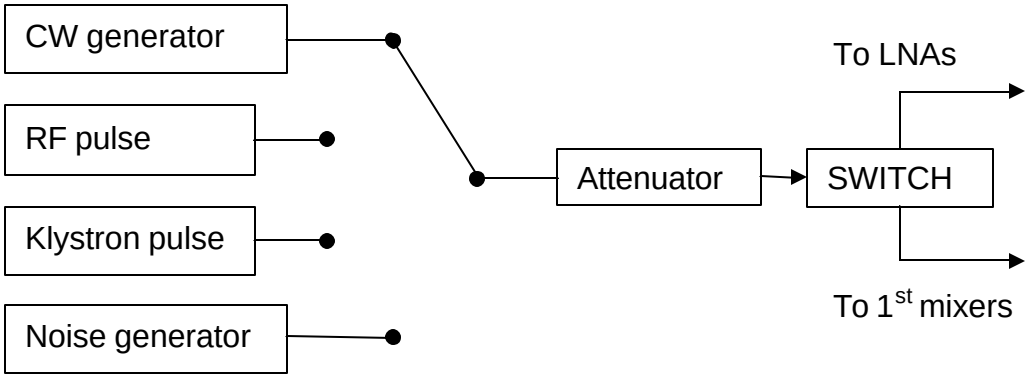

Fig. 2.10 Block diagram of existing calibration circuit on the WSR-88D.

As was indicated in section 2.3.2, the coherent leakage complicates calibration of differential reflectivity if the CW generator is used. We have found several places where the leakage showed up. Witch was in the switch!, and our angel told us to use the noise generator. We have terminated the path to the mixer (at the switch) to reduce the leakage but it was not sufficient. Then there is leakage within the attenuator which was harmful

only if we use the CW generator. Note that in case of coherent leakage the voltage of the CW generator and the leakage voltage add so that the effect is very strong, much more so than if the powers were additive! Rather than fight this problem we have found a way around it which is robust, repeatable, and produces differential reflectivity with error smaller than 0.1 dB.

Measurements should be made on the preproduction WSR-88D to determine if similar results apply and if coherent leakage is a factor.

3. Other Possibilities

Another method to calibrate differential reflectivity is briefly reviewed. It is suitable for sequential H,V transmission and could be adapted to the SHV mode.

3.1 Sequential transmission of H and V polarization

Hubbert et al. (2003) suggest a way to calibrate differential reflectivity using natural scatterers. The method is well suited for radars that transmit sequential linear polarizations, such as CSUCHILL. The essence of the proposed calibration is to use sun scan for calibrating the receiving path and use cross polar measurement for calibrating the transmit path including the transmitted powers. In Fig. 3.1 is a schematic which will

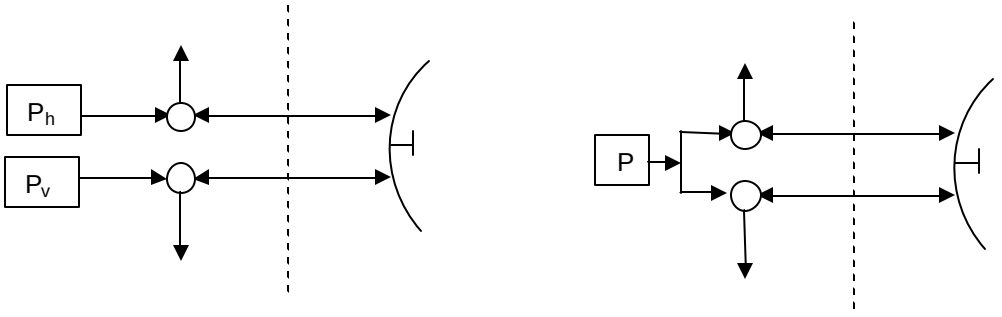

Fig. 3.1 Schematic for calibration of differential reflectivity, adapted from Hubbert et al, (2003), but simplified.

be used to summarize this technique. The P_h and P_v are powers at horizontal and vertical polarizations; these are transmitted sequentially. The total losses on transmit at the two polarizations are denoted as L_{hT} and L_{vT} whereas the gains on receive are G_{hR} and G_{vR}. So the L_{hT} includes losses up to and including the circulator, then to the antenna, and the gain

of the antenna G_h all for horizontal polarization! Subscript h stands for horizontal and T is in the transmit chain.

The measured differential reflectivity Z_{drm} at the output of digital receiver is related to the intrinsic values Z_{dr} with

$$Z_{drm} = \frac{P_h L_{hT} G_{hR}}{P_v L_{vT} G_{vR}} Z_{dr} . \qquad (3.1)$$

Clearly the bias is $(P_h L_{hT} G_{hR})/(P_v L_{vT} G_{vR})$. Hubbert et al. (2003) propose two measurements to compensate for this bias. One measurement is from the sun. Because the sun is wideband the measurement will contain the integral effect over the bandwidths. Thus let the ratio of horizontally polarized power to the vertically polarized powers from the sun be

$$S = \frac{G_{vR} \int H_{vR}(f) df}{G_{hR} \int H_{hR}(f) df}, \qquad (3.2)$$

where the power transfer functions $H_{hR}(f)$ and $H_{vR}(f)$ are normalized so that $H_{hR}(0) = H_{vR}(0) = 1$. These transfer functions are at the base band after down conversion (see appendix C).

The other needed measurement is the ratio of cross polar powers. In a sequential transmission these powers are obtained simultaneously. By reciprocity the cross-polar backscatter cross sections are equal. Therefore the ratio of powers for a horizontally transmitted and vertically received signal (P_{vh}) to the vertically transmitted and *horizontally* received signal is

$$P_{vh}/P_{hv} = P_h L_{hT} G_{vR} / P_v L_{vT} G_{hR}. \qquad (3.3)$$

Note that the radar return is narrow band hence there are no bandwidth effects on the Z_{dr} measurement, only the difference in gains (G_{hR} and G_{vR}) causes the bias.

By combining (3.2) and (3.3) the bias term next to the intrinsic Z_{dr} (3.1) becomes

$$\text{Bias} = (P_{vh}/P_{hv}) (G_{vR}/G_{hR})^2. \qquad (3.4)$$

The ratio (G_{vR}/G_{hR}) can be obtained from sun measurement (3.2) *only if the overall frequency transfer functions $H_{hR}(f)$ and $H_{vR}(f)$ are identical.* On the KOUN the integral difference between the two is less than 0.05 dB, hence it is not a factor. Because in (3.4) the ratio is squared the net effect is twice as large or 0.1 dB. To determine the difference on other WSR-88Ds requires measurement with noise and signal generators as suggested in this report.

The bias (3.4) takes account of the transmitted difference in powers and is made from two measurements at the output of the digital receivers. Still noises in the two channels have to be measured and appropriately subtracted. Further, the measurement is at two different power levels; one is the power from the sun the other is the power level of the cross polar components. There may be bias in Z_{dr} between these two values which

can be estimated quite well by the method described in section 2. Therefore, automatic calibration over the full dynamic range of receiver is still required at the end of each volume scan. On top, one might have to account for the difference between the wideband (sun) source and the narrowband cross-polar echo powers as explained in section 2 and in the Appendix C.

3.2 Simultaneous transmission and reception, SHV mode

In this mode the transmitter power is split (Fig. 3.1 b) hence the direct application of the scheme by Hubbert et al. (2003) needs to be modified. Whether such scheme would be available depends on the chosen configuration for the transmitting chain. If the SHV becomes the only available mode, cross polar measurement would be impossible. There are no compelling reasons to include cross polar measurements. Nonetheless there might be reasons to revert to the previous capability which is transmission of H only and reception of H (and V if desired). Such configuration is implemented on the KOUN radar.

In Fig. 3.2 plotted is a possible hardware configuration for the SHV scheme. It is equivalent (but not identical) to the one implemented on the KOUN and contains the minimum number of switches (one) with which one can have the SHV mode and the mode for transmitting H and receiving both. This scheme precludes measurement of the horizontal cross-polar component (which is also unavailable on the KOUN radar).

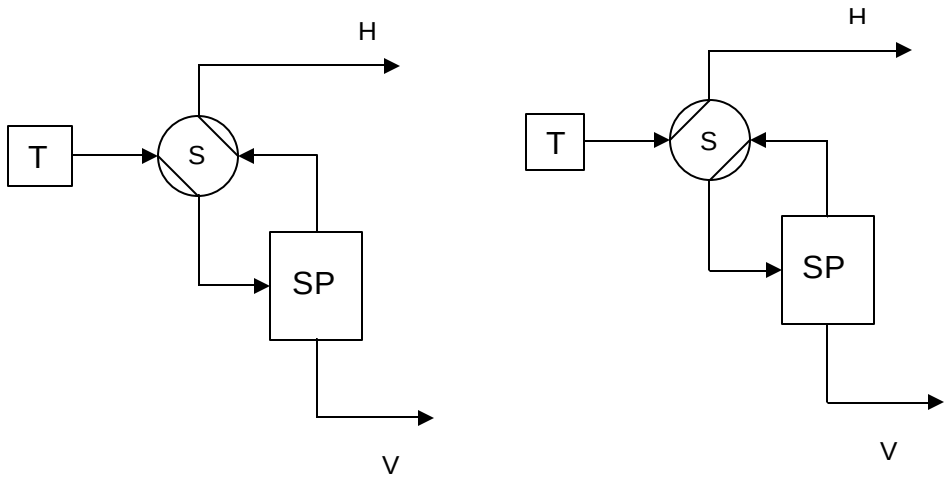

(a) (b)

Fig. 3.2 Configuration for transmission of simultaneous H and V signal; S is a four port microwave switch and SP is the power splitter. The lines within the switch indicate which input ports are connected and the switch rotates 90^o into its second position. Connection in (a) enables the flow from transmitter to the power splitter and then into the H and V waveguides. Position in (b) is for transmission of H waves. The circulators and receiver channels are not shown, but would connect to the H and V lines.

The configuration in Fig. 3.3 with two switches makes possible the SHV mode, the mode for transmission of H, and the mode for transmission of V. Hence both cross-polar powers can be estimated.

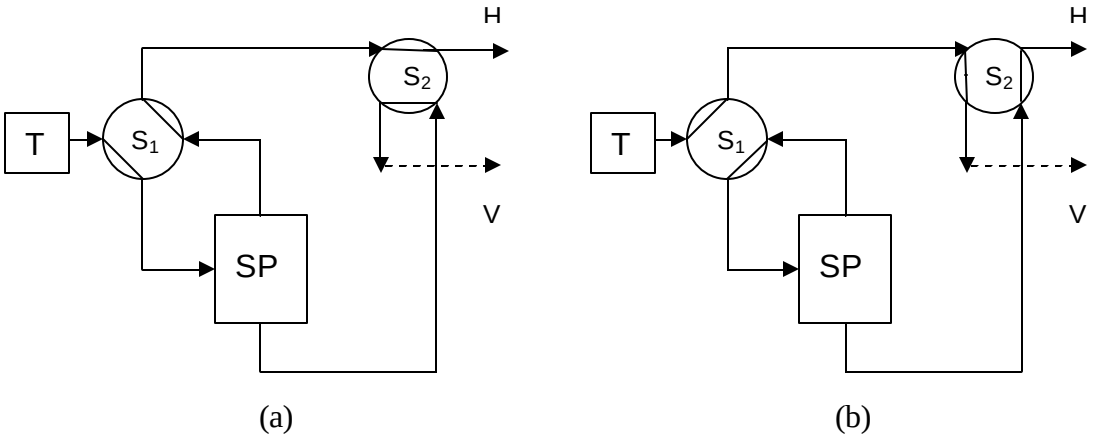

Fig. 3.3 Configuration of the transmission channels with two switches, S_1 and S_2 that allows (a) simultaneous SHV mode as well as (b) two modes for cross polar measurement. Dashed line indicates that there is no connection at the cross over point.

If the switches are as in Fig. 3.3 a), the radar is in the SHV mode. If the position of S_1 is as in Fig. 3.3 b) the radar transmits V (and receives both). To transmit H the S_2 has to be turned to its second position, and then the cross-polar V component can be measured. Although from these cross polar components a good part of the system Z_{dr} can be calibrated one component is left out! That is the power splitter. Its differential power must be measured. These considerations and the added complexities brought by the switches lessen the appeal of such calibration for the SHV mode, especially since a simpler and straight forward method demonstrated in this report is more than adequate.

4. Conclusions

A procedure for calibrating differential reflectivity has been developed and tested on the KOUN polarimetric radar. At its essence is separation of the bias into a constant part and time varying part (due to active receiver components). It proceeds as follows.

- Constant part is measured at the time of retrofit and is due to the transmitter path and part of the receiver path.
- Transmitter path is measured at the couplers above the elevation rotary joints using the transmitted signal.
- Receiver path consists of two pairs of measurements. One pair uses internal noise generator, sun scan, and again the noise generator to establish the difference between the outside of radome and the LNAs inputs. The other pair uses the internal CW generator, external signal generator, and again the internal CW generator to measure the difference between the elevation rotary joints and the LNAs inputs.

- From the differences in the receiver path one computes the part between the elevation rotary joints and the outside of radome.

- The time varying part must be updated at the end of each volume scan.

- The total bias is the sum of constant and time varying parts.

Overall there are four measurements, one in the transmission path and three in the receiving path. We have shown that each of the measurement has rms error smaller than 0.04 dB, hence the total is less than 0.08 dB.

The recommended procedure can achieve errors within 0.1 dB, if caution and care is exercised such that: 1) all differences in coupling losses are accounted for, 2) noises are correctly estimated and subtracted from the H and V powers, 3) some measurements are repeated or bracketed by a companion measurement, and 4) high quality equipment is used.

Assuming that the quality of upgraded WSR-88D is equal or better than that of the KOUN, the procedure tested herein is directly transferable. It was written by city dudes aiming for village sages to replicate it without the benefit of algorithm description languages. Nonetheless, similar measurements must be made on the preproduction model to determine its characteristics. First, all the essential couplers must be present on the preproduction model. The leakage must be quantified and the bias characteristic over the full dynamic range must be measured to determine if our procedure is applicable verbatim. Most measurements must be automated and under computer control. This applies to those with internal CW and noise generators, and to sun scans. Measurement with the external generator attached to couplers above the El rotary joints should be semi automated so that the results from the output of the digital receiver are immediately available. Computer routines for initial calibration should be developed such that coupler losses, number of samples for averaging, noise powers, etc., can be appropriately inserted. The essential part of calibration for end of volume scan must be automated within the volume coverage patterns (VCPs). With such automation the drift in differential gain can be eliminated almost all the time.

Exception, on the KOUN about once in ten hours there is a significant step change in differential gain. Such abrupt change would be missed in one volume scan so that the Z_{DR} could be off by about 0.5 dB. Nonetheless, calibration for the subsequent volume scan would redress this immediately. Measurements must be made on the prototype dual polarization WSR-88D to determine if similar problem exist.

Because absolute calibration of reflectivity within 1 dB is still hard to achieve it will appear to casual readers that our claim of 0.1 dB accuracy is exaggerated. The principal reason that this is not so, is that the essence of the measurement is in relative comparisons of the two channels! Because the transmitted power is split, on transmit the relative difference is constant and what remains is to continuously track the relative difference in the receiver gains.

Appendix A - Bandwidth effects

The weather signals in range time are broad band and have a frequency transfer function shaped by the receiver. Therefore, for calibration purposes, measurement with the sinusoid from the signal generator might not be directly applicable (with no adjustments) to the weather signal. This, however, is not the case for the sun signal which is broad band. Thus, if the frequency characteristics of the two chains differ the measured differential reflectivity from the sun and with the signal generator might differ (such was the case on the Sigmet's RVP7 system). This is one reason that we have paired the noise generator with the measurement from the sun. The other reason is to avoid leakage associated with the CW internal generator.

If the frequency transfer functions of the two receiver chains differ (as was the case in our implementation of the dual polarization with the RVP7 signal processor) there would be effects on calibration of differential reflectivity. (There are no such differences in the implementation with the RVP8 processor.) These are explained herein.

Consider the block diagram in Fig. 2.4 and denote the frequency transfer functions for the powers at horizontal and vertical polarizations as follows.

Point 3 to 4, from the coupler before the LNA to the output of digital receiver, for horizontal polarization the transfer is $G_{3h}H_{3h}(f)H_{mh}(f)$; for vertical it is $G_{3v}H_{3v}(f)H_{mv}(f)$. H_3 stands for the analogue part of the transfer function. It includes the receiver protector, and all the filters between the LNA and the digital receiver. H_m is the digital matched filter. Assume that the two digital filters have identical responses so that $H_{mh}(f) = H_{mv}(f)$. The frequencies are referenced to zero at base band, but come from the carrier which has been down converted. Further it is implied that

$$H_{3h}(0)H_{mh}(0) = H_{3v}(0)H_{mv}(0) = 1. \qquad \text{(A.1)}$$

Obviously the gain factors are related to the bias $?_{34}$ by

$$?_{34} = 10 \log\{[G_{3h} \int H_{3h}(f)H_{mh}(f)df] / [G_{3v} \int H_{3v}(f)H_{mv}(f)df]\}. \qquad \text{(A.2)}$$

But, with the sinusoidal signal generator the ratio of gains G_{3h}/G_{3v} is measured, which might not (like in the case of RVP7) equal to (A.2).

Point S to 3, from outside the radome to the coupler before the LNA. For horizontal polarization the transfer function is $G_{S3h}H_{S3h}(f)$ and for vertical it is $G_{S3v}H_{S3v}(f)$. Again let the frequency be down converted to base band and the normalization

$$H_{S3h}(0) = H_{S3v}(0) = 1, \qquad \text{(A.3)}$$

allows separation of the bandwidths from the gain effects. The bias between the outside (sun) and the LNA is given by

$$?_{S3} = 10 \log(G_{S3h} \int H_{S3h}(f)df / G_{S3v} \int H_{S3v}(f)df). \qquad \text{(A.4)}$$

From the sun scan and with the internal noise generator we measure

$$\frac{G_{S3h}\int H_{S3h}(f)H_{3h}(f)H_{mh}(f)df\int H_{3v}(f)H_{mv}(f)df}{G_{S3v}\int H_{S3v}(f)H_{3v}(f)H_{mv}(f)df\int H_{3h}(f)H_{mh}(f)df}. \qquad \text{(A.5)}$$

The products of three frequency transfer functions in the integrands of (A.5) correspond to the measurement from the sun and the products of two transfer functions are measured with the noise generator. The gain parts have canceled out perfectly and we show next that the integrals for all practical purposes should cancel as well.

The bandwidth of the frequency response from the coupler before the LNA and the output of the matched filter (in either channel) is at least an order of magnitude smaller than the bandwidth of the circuit from the antenna to the coupler. Therefore $H_{S3h}(f)$ and $H_{S3v}(f)$ have values close to 1 (valid at and near zero frequency). Then the integrals of the frequency responses almost cancel out and the Z_{dr} approximately equals to the ratio of gains.

Upon measurement we found that the difference between Z_{dr} measured with a broadband noise and narrowband signal (both from above El joints) is less than 0.06 dB (quantization interval on the RVP8's, A-scope). This is to be expected because the frequency transfer functions of the two receivers are primarily shaped by the digital filters. Unlike in analogue matched filters which could differ due to component variability the digital ones are identical and therefore do not cause difference between measurements with a sinusoidal and noise sources.

Appendix B – Temporal variation of bias

The fundamental premise behind the suggested automatic calibration scheme is that the time variation of bias in differential reflectivity is slow compared to the volume update time. That way the correction would follow the drift and keep bias within acceptable bounds. Herein we report measurements of differential reflectivity over extended periods of time and demonstrate that most of the time the correction should be very good.

We start with the differential gains (i.e., Z_{DR}) of RVP8 (Fig. B.1). Power from a signal generator (57 MHz) was split and supplied directly to the RVP8. For almost 8 hours the differential reflectivity was recorded. The maximum variation over this time is 0.02 dB. Clearly the variations caused by the digital receiver are insignificant.

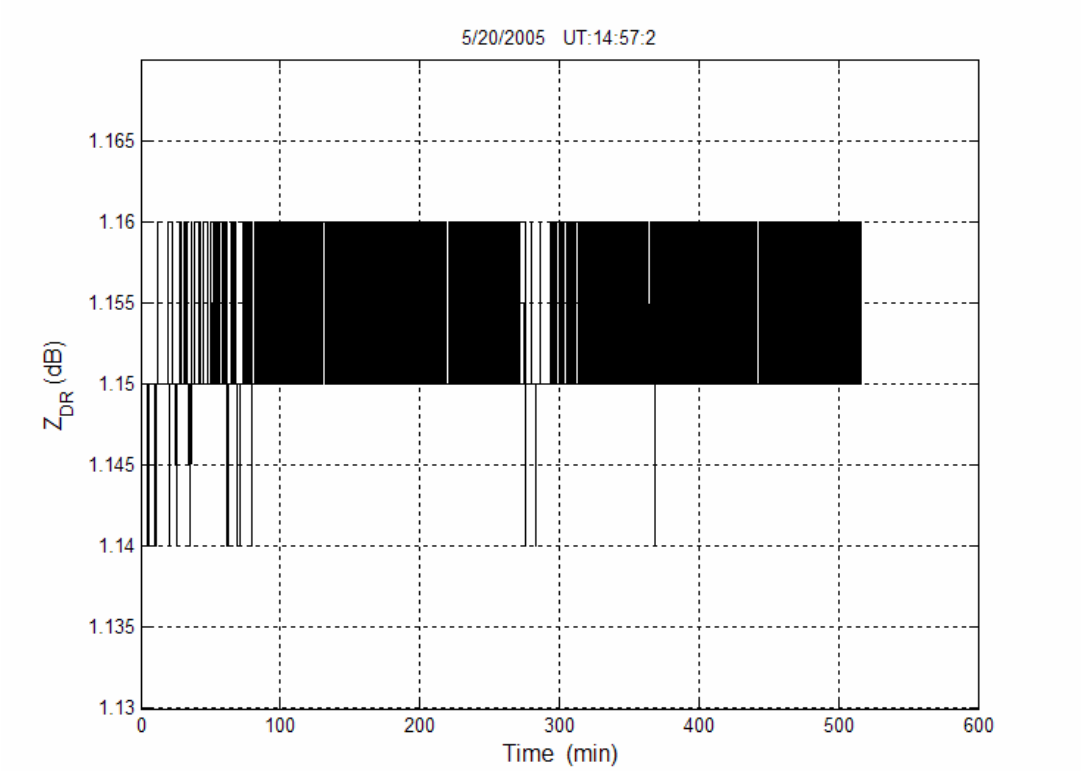

Fig. B.1 Time record of differential reflectivity measured at the output of RVP8. Input was at intermediate frequency and at the two channels of RVP8. Beginning time of the measurement is indicated in the title.

Next the power from the RF generator was split and supplied to the mixer preamplifiers. The record of differential reflectivity was very stable.

Last the power was injected to the calibration port. Differential reflectivity vs time (Figs. B.2a, b) exhibits a very sharp discontinuity (~0.7 dB) over a few min interval.

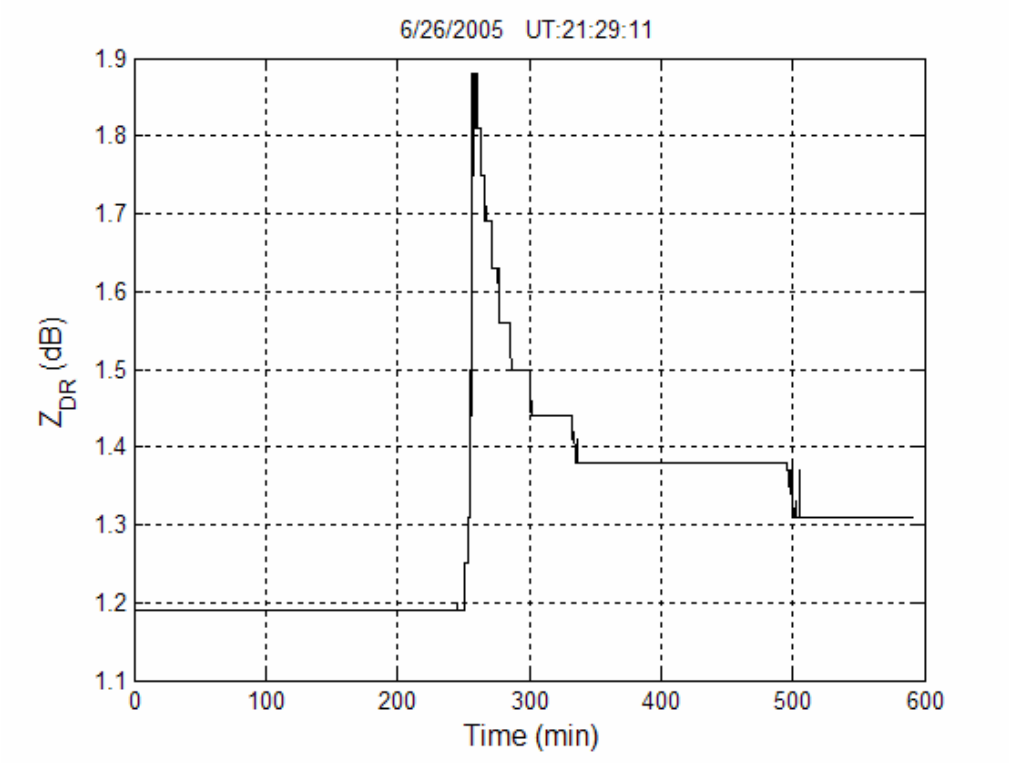

a)

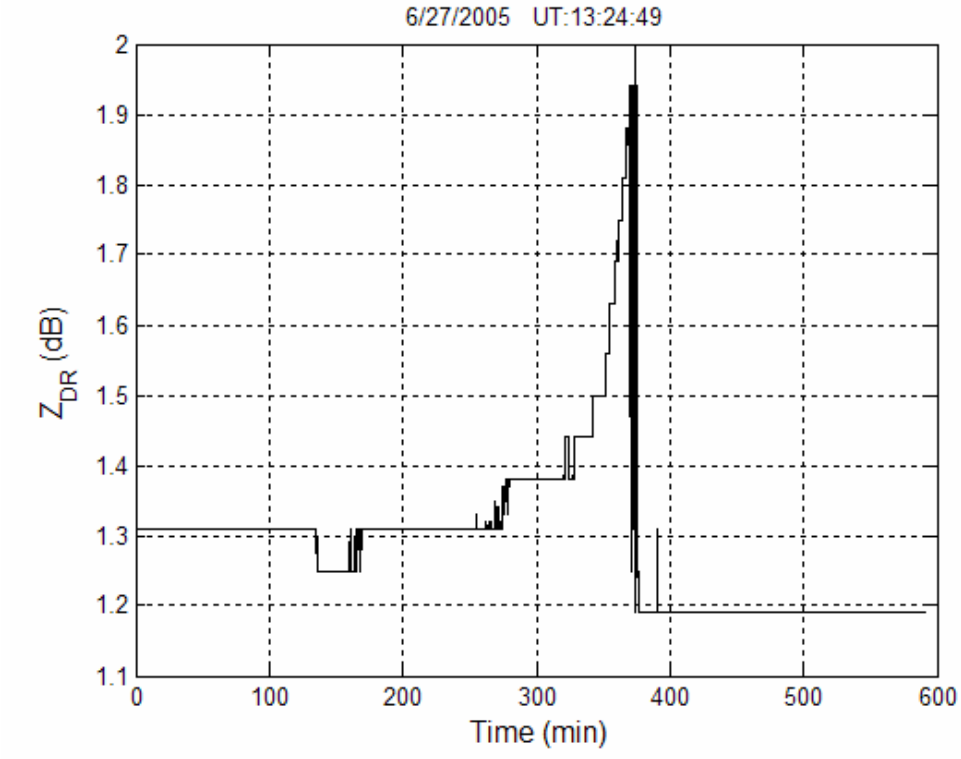

b)

Fig. B.2 Differential reflectivity bias between the LNAs and the digital receiver outputs vs time: a) on June 26, and b) on June 27 2005; beginning times are in the titles.

The discontinuity is either followed or preceded by a “more gradual” change. Because the “more gradual” change has discontinuities of less than about 0.1 dB, automatic calibration would capture these changes. The large discontinuity would be missed somewhere in one volume scan but it would be neutralized by the automatic calibration in the next volume scan. We conclude that the source is in the LNAs. It could be that there are regulating circuits (for temperature or power) which activate if the variable is out of accepted range; at activation time there is a sharp change in the gain of one or both LNAs. It is likely that activation brings the system to a new operating point; after that forcing is turned off and the system drifts slowly back to previous equilibrium.

Appendix C – Transfer characteristics of the RVP8: Power and differential reflectivity

Herein we document some details of the transfer characteristic of power and differential reflectivity. An intermediate frequency (IF) generator was connected directly to the RVP8 and output powers (in internal RVP8 units) were recorded (also the attenuations at the input were recorded but are not shown here). For the powers we plot the difference between the fitted linear lines as in Fig. 2.8 and actual measurements. The result is in Fig. C.1. The trend over full dynamic range is less than 0.3 dB and maximum fluctuations are smaller than 0.2 dB, both well within the 1 dB specs.

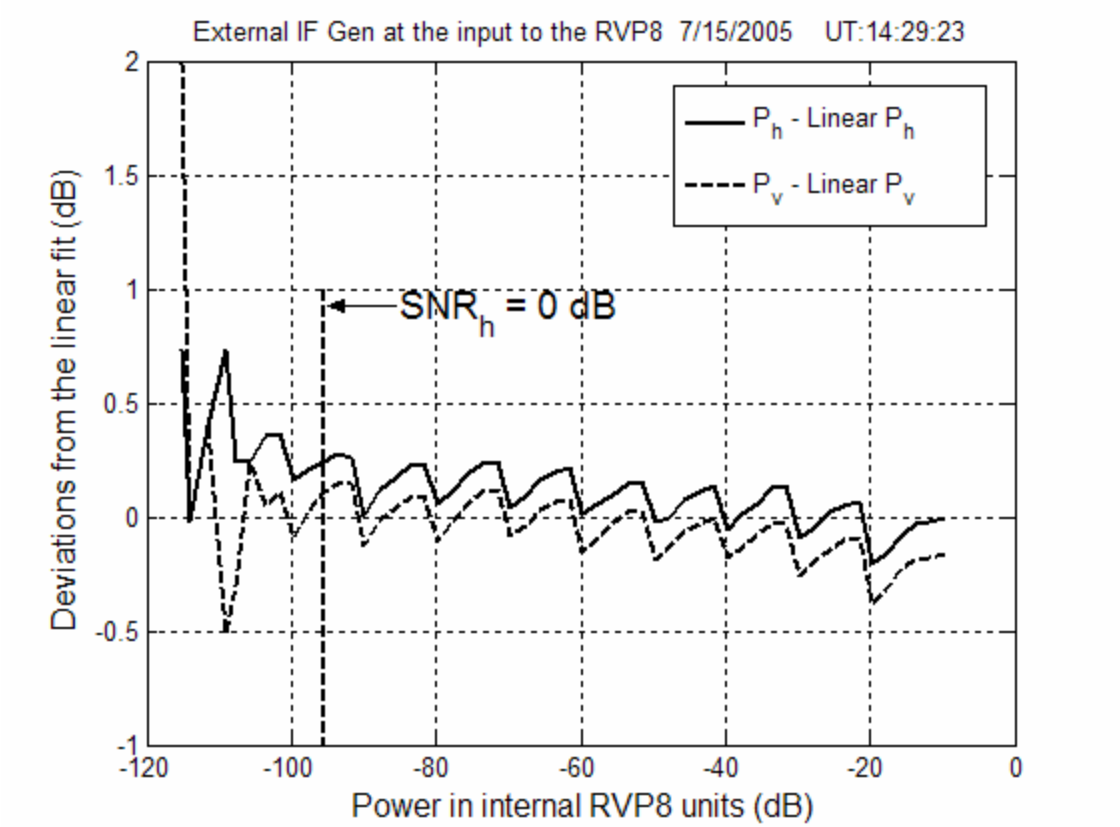

Fig. C.1 Deviations of the powers from linear at the output of the RVP8 and in units internal to that processor.

The transfer functions of differential reflectivity, measured on two days are plotted in Fig. C2. Remarkable similarity in details suggests that the hardware is stable, and measurements are repetitive. The trend is also less than about 0.03 dB and the rms fluctuations are below 0.02 dB. Note that the RVP8 is only one part of the system. The linear fit of the total transfer has a smaller trend and about the same fluctuations as on the RVP8. Clearly the precision with which we can measure differential reflectivity is better than 0.1 dB.

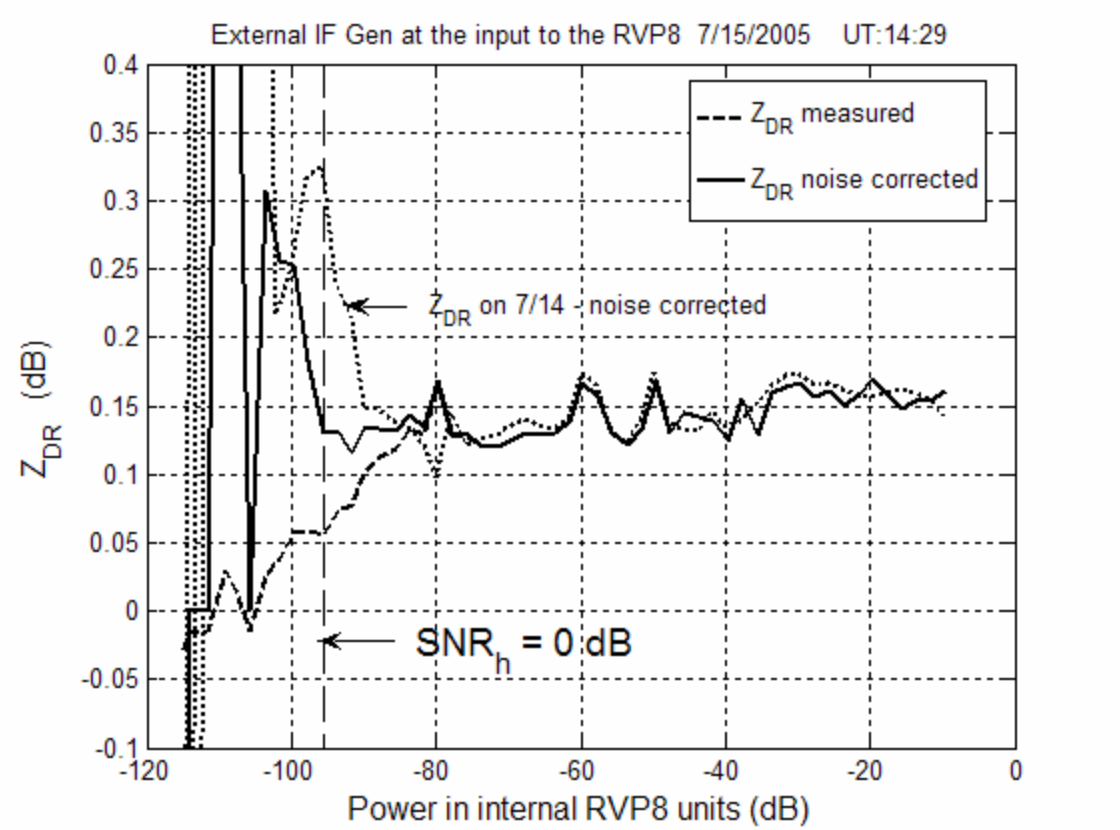

Fig. C.2 Differential reflectivity bias within the RVP8. Data were obtained on two consecutive days. Z_{DR} curves denoted in the text box are from 7/15 and the doted curve was obtained on 7/14, 2005.

References

Hubbert, J.C., V.N. Bringi, and D. Brunkow, 2003: Studies of the polarimetric covariance matrix. Part I: Calibration methodology. *Jour. Atmos. Ocean. Tech.*, **20,** 696-706.

Melnikov, V.M., D. S. Zrnic, R. J. Doviak, and J. K. Carter, 2003: Calibration and Performance Analysis of NSSL's Polarimetric WSR-88D, NOAA/NSSL Report, 77 pp.

Zrnic, D.S., Melnikov, V. M., and A. V. Ryzhkov, 2005: Polarimetric properties of ground clutter. Submitted to *Jour. Atmos. Ocean. Tech.*

Zahrai, A., and D.S. Zrnic, 1993: The 10-cm-wavelength polarimetric weather radar at NOAA's National Severe Storms Laboratory, Zahrai, A., and D. S. Zrnic, *Jour. Atmos. Ocean. Tech.***, 10**, 649-662.

LIST OF NSSL REPORTS FOCUSED ON POSSIBLE UPGRADES TO THE WSR-88D RADARS

Torres S., M. Sachidananda, and D.S. Zrnic, 2004: Signal Design and Processing Techniques for WSR-88D Ambiguity Resolution: Phase coding and staggered PRT, implementation, and clutter filtering. NOAA/NSSL Report, 157 pp.

Melnikov, V. M, and D.S. Zrnic, 2004: Simultaneous transmission mode for the polarimetric WSR-88D – statistical biases and standard deviations of polarimetric variables. NOAA/NSSL Report, 84 pp.

Bachman, S., 2004: Analysis of Doppler spectra obtained with WSR-88D radar from non-stormy environment. NOAA/NSSL Report, 86 pp.

Torres S., D. Zrnic, and Y. Dubel, 2003: Signal Design and Processing Techniques for WSR-88D Ambiguity Resolution: Phase coding and staggered PRT, implementation, data collection, and processing. NOAA/NSSL Report, Part 7, 128 pp.

Schuur, T., P. Heinselman, and K. Scharfenberg, 2003: Overview of the Joint Polarization Experiment (JPOLE), NOAA/NSSL Report, 38 pp.

Ryzhkov, A, 2003: Rainfall Measurements with the Polarimetric WSR-88D Radar, NOAA/NSSL Report, 99 pp.

Schuur, T., A. Ryzhkov, and P. Heinselman, 2003: Observations and Classification of echoes with the Polarimetric WSR-88D radar, NOAA/NSSL Report, 45 pp.

Melnikov, V. M, D. S. Zrnic, R. J. Doviak, and J. K. Carter, 2003: Calibration and Performance Analysis of NSSL's Polarimetric WSR-88D, NOAA/NSSL Report, 77 pp.

NCAR-NSSL Interim Report, 2003: NEXRAD Range-Velocity Ambiguity Mitigation SZ(8/64) Phase Coding Algorithm Recommendations.

Sachidananda, M., 2002: Signal Design and Processing Techniques for WSR-88D Ambiguity Resolution, NOAA/NSSL Report, Part 6, 57 pp.

Doviak, R. J., J. Carter, V. Melnikov, and D.S. Zrnic, 2002: Modifications to the Research WSR-88D to obtain Polarimetric Data, NOAA/NSSL Report, 49 pp.

Fang, M., and R. J. Doviak, 2001: Spectrum width statistics of various weather phenomena, NOAA/NSSL Report, 62 pp.

Sachidananda, M., 2001**:** Signal Design and Processing Techniques for WSR-88D Ambiguity Resolution, NOAA/NSSL Report, Part 5, 75 pp.

Sachidananda, M., 2000**:** Signal Design and Processing Techniques for WSR-88D Ambiguity Resolution, NOAA/NSSL Report, Part 4, 99 pp.

Sachidananda, M., 1999: Signal Design and Processing Techniques for WSR-88D Ambiguity Resolution, NOAA/NSSL Report, Part 3, 81 pp.

Sachidananda, M., 1998: Signal Design and Processing Techniques for WSR-88D Ambiguity Resolution, NOAA/NSSL Report, Part 2, 105 pp.

Torres, S., 1998: Ground Clutter Canceling with a Regression Filter, NOAA/NSSL Report, 37 pp.

Doviak, R. J. and D. S. Zrnic, 1998: WSR-88D Radar for Research and Enhancement of Operations: Polarimetric Upgrades to Improve Rainfall Measurements, NOAA/NSSL Report, 110 pp.

Sachidananda, M., 1997: Signal Design and Processing Techniques for WSR-88D Ambiguity Resolution, NOAA/NSSL Report, Part 1, 100 pp.

Sirmans, D., D. S. Zrnic, and N. Balakrishnan, 1988: Doppler radar dual polarization considerations for NEXRAD, NOAA/NSSL Report, Part II, 70 pp.

Sirmans, D., D. S. Zrnic, and M. Sachidananda, 1986: Doppler radar dual polarization considerations for NEXRAD, NOAA/NSSL Report, Part I, 109 pp.